

1 **Global forest dataset incongruence creates high uncertainties for conservation, climate, and**
2 **development policy**

3 Sarah E. Castle,^{1,2,3*,†} Peter Newton,⁴ Johan A. Oldekop,⁵ Kathy Baylis,⁶ and Daniel C.
4 Miller^{7,8,9**}

5 ¹Natural Resources and Environmental Sciences, University of Illinois Urbana-Champaign,
6 Urbana, Illinois, USA.

7 ²Yale School of the Environment, Yale University, New Haven, Connecticut, USA.

8 ³Department of Forest and Wildlife Ecology, University of Wisconsin-Madison, Madison,
9 Wisconsin, USA.

10 ⁴Department of Environmental Studies, University of Colorado Boulder, Boulder, Colorado,
11 USA.

12 ⁵Global Development Institute, University of Manchester, Manchester, UK.

13 ⁶Department of Geography, University of California Santa-Barbara, Santa-Barbara, California
14 USA.

15 ⁷Keough School of Global Affairs, University of Notre Dame, Notre Dame, Indiana, USA.

16 ⁸Basque Center for Climate Change (BC3), Leioa, Bizkaia, Spain

17 ⁹University of Deusto, Bilbao, Bizkaia, Spain

18

19 *Correspondence (lead contact): castle3@wisc.edu

20 †Current address: Department of Forest and Wildlife Ecology, University of Wisconsin-Madison,
21 Madison, Wisconsin, USA.

22 **Correspondence: dmille33@nd.edu

23

24 **Summary**

25 Forests are central to climate, biodiversity, and development goals, but effective monitoring and
26 evaluation of their contributions depends on reliable data. Satellite-derived global forest cover
27 and change datasets (GFDs) are widely used to address this need. However, differences in
28 resolution, forest definition, and methodology challenge their use in research and policy. Yet
29 how GFD differences affect key forest-related estimates remains poorly understood. Here, we
30 quantify global area-based spatial congruence among ten GFDs and test their influence on three
31 national policy-relevant estimates: carbon accounting, forest-poverty mapping, and biodiversity
32 habitat. We find only 26% spatial congruence among GFDs at native resolution. This low
33 congruence translates to an order-of-magnitude difference in national case study indicator
34 estimates. We demonstrate that GFD selection fundamentally shapes monitoring and evaluation
35 outcomes, particularly in biomes with fragmented or sparse tree cover. We provide a decision-
36 support framework to guide GFD selection according to different forest-related science and
37 policy applications.

38 **Keywords:** forest policy, sustainable development, conservation, climate change, poverty,
39 remote sensing

41 **Introduction**

42 Forests are critical ecosystems that provide multiple services essential to achieving global
43 sustainability goals. They are key to climate change mitigation both through carbon uptake
44 (sequestering roughly 15.6 billion metric tons of CO₂ each year) and reduced emissions through
45 avoided deforestation (since deforestation, fire, and disturbance release roughly 8.1 billion metric
46 tons of CO₂ each year)¹. Forests are essential for biodiversity, providing habitat for the majority

47 of terrestrial species, including roughly 80% of amphibian species, 75% of bird species, and 68%
48 of mammal species – along with housing approximately 60,000 different tree species². Beyond
49 these critical ecological functions, forests directly support the livelihoods and resilience of over
50 1.6 billion people worldwide, many of whom are among the global poor³. These central roles in
51 climate, biodiversity, and livelihoods mean that forest ecosystems are fundamental to major
52 international policies and finance mechanisms, including the Paris Agreement, the Kunming-
53 Montreal Global Biodiversity Framework, and many United Nations 2030 Sustainable
54 Development Goals (SDGs)^{2,4,5}. Consequently, national governments, non-governmental
55 organizations, and private sector investors actively rely on accurate, timely data on the extent of
56 forest conservation, deforestation, and reforestation to track progress, allocate resources, enforce
57 regulations, and inform more just and effective sustainability policy.

58 Satellite-derived global forest datasets (GFDs) have become a dominant source of
59 information for large-scale forest monitoring, often replacing costly and time-consuming ground-
60 based inventories. The rapid rise in GFDs generated with increasingly advanced remote sensing
61 and machine learning techniques, together with high-performance, cloud-based geospatial
62 platforms, offers unparalleled access to high-resolution, globally available data. This
63 unprecedented access has led to wide adoption of GFDs by researchers, policymakers, and
64 practitioners for a range of uses. For example, numerous empirical studies have quantified how
65 forest conservation policies reduce deforestation (e.g. Börner et al. ⁶), support local livelihoods
66 (e.g., Ordóñez et al. ⁷), and generate climate-relevant carbon offsets when properly designed
67 (e.g., West et al. ⁸).GFDs are especially important for applications in countries where there is a
68 lack of high-quality, recently updated, national or regional land cover datasets. Relatively few
69 countries or regions have publicly available datasets that could be used as alternatives, with

70 notable exceptions including Brazil⁹, North America^{10,11}, Europe^{12,13}, and China^{14,15}. In many
71 cases, however, regional or national data may not be readily available or may have different
72 limitations than the GFD (e.g., different classification errors or not available annually).

73 Despite their widespread use, GFDs are not interchangeable: they vary significantly in
74 spatial resolution, forest definition, classification methodology, model training procedures, and
75 temporal consistency and span. Prior work has demonstrated several conceptual and technical
76 variations in global land cover and forest cover datasets¹⁶⁻²⁰, even as these same products have
77 underpinned high-impact evaluations of conservation programs^{6,21} and econometric studies
78 linking land-cover change to economic outcomes^{22,23}. These variations – for example, a dataset
79 classifying forest as pixels with 30% tree canopy cover versus 10% tree canopy cover – have
80 been shown to change the estimated extent of forests from 35% to 22% of the world’s land area
81 ¹⁷. These differences ultimately dictate which forests are counted, and how they are represented
82 in climate finance, measurements of forest-based livelihoods, and tracking progress towards
83 biodiversity conservation goals. However, the practical implications of GFD discrepancies for
84 quantitative social and environmental policy questions remain undertested.

85 The uncertainty arising from this data incongruence presents a challenge to evidence-
86 based conservation and development action. Although recent studies have quantified the
87 classification accuracy of several recent, high-resolution GFDs (e.g., Xu et al. ²⁴), the extent of
88 spatial disagreement among them and other widely used GFDs, both in terms of mapped forest
89 extent and location, has not been systematically characterized. The choice of GFD can determine
90 whether a region is prioritized for climate and biodiversity financing, or whether people’s forest-
91 related livelihoods are captured by governing bodies. These challenges are particularly
92 noticeable in biomes with sparse or fragmented tree cover, where forest extent is highly sensitive

93 to forest class definitions. Here, we quantify how GFD choice propagates uncertainty into real-
94 world assessments.

95 We shed light on how the conclusions decision makers and researchers draw about the
96 status and changes in the world's forests may be heavily influenced by their choice of GFD. We
97 do so by first assessing whether and how different GFDs affect estimates of forest extent. We
98 quantify spatial congruence (i.e., area of agreement in forest classification) between the eight
99 most used GFDs that measure forest cover at single points in time (see Methods and Table S1 for
100 details). Then, by overlaying two global change products and the eight static maps in three
101 illustrative case-studies (Kenya's forest carbon, forest-poverty mapping in India, biodiversity
102 habitat in Brazil), we show how choice of GFD can alter downstream estimates by up to an order
103 of magnitude. We compare datasets based on their published forest class definitions, which differ
104 substantially in biophysical thresholds and classification logic and do not reflect a standard forest
105 land use definition (e.g., FAO ²⁵). Most global forest datasets apply a biophysical definition of
106 forest, typically based on minimum tree canopy cover, tree height, and/or vegetation type
107 thresholds. We use the term "forest cover" when referring to forest land cover classes in GFD
108 products¹⁷.

109 Our aim is to quantify spatial congruence across available GFDs and to provide
110 illustrative examples of how differences in forest representation, under each dataset's own
111 published methodology and forest definition, affect downstream sustainability-relevant analyses.
112 While sample-based area estimation is the recommended standard for unbiased national
113 estimates^{26,27}, our comparative approach provides a complementary perspective relevant to many
114 researchers and practitioners who use GFD products directly in ecological, social, or policy
115 studies.

116

117 **Results**

118 *Spatial agreement of forest cover data*

119 The eight forest cover datasets exhibited low overall agreement (Figs. 1 and 2). Of the
120 total (or union) of the area classified as forest by at least one dataset (6.8 billion ha), only 26%
121 was classified as forest by all eight datasets. Systematic pairwise comparison of each of the
122 eight datasets revealed that some datasets agreed strongly with one another while others
123 overestimated or underestimated forest extent relative to others (Figs. 2 and S3). CGLC had the
124 highest pairwise agreement with the other datasets, while MODIS-IGBP, followed by ESA-C3S,
125 had the lowest pairwise agreement with the others. Withholding MODIS-IGBP, the spatial
126 congruence was still only 35% among the other seven datasets (Table S2). When we included
127 savanna classes for the MODIS-IGBP dataset (Fig. S1), agreement among the eight GFD
128 increased to 35%, suggesting that savannas and savanna-forest transitions were sometimes
129 classified as forest due to the characteristically sparse tree canopy cover commonly found in
130 these ecosystems.

131 Differences in classification were most apparent at finer-grained spatial scales. Some
132 datasets classified large swaths of fragmented tree cover and mosaic landscapes as entirely
133 forested. Some datasets captured smaller forested patches and linear tree features, whereas others
134 missed these (Fig. 1b). Based on visual inspection across multiple global locations, ESA-WC and
135 GLAD-LCLUC appeared comparatively better at capturing small patches and linear features.
136 While Figure 1b provides one illustrative example, this is a qualitative observation and does not
137 represent a formal or systematic evaluation. Additionally, we show that, as expected, areas with
138 lower tree canopy cover have much lower spatial congruence than areas with high levels of tree

139 canopy cover (Fig. S2, Table S3). We would not expect to have full agreement for low tree cover
140 due to differences in forest definition among the datasets: only five of the eight would capture
141 sparse canopy cover forests, so Fig. S2 and Table S3 should be interpreted accordingly.

142 To reduce the effects of differing native resolutions across datasets, we aggregated all
143 GFDs to a common 500-meter resolution (see Methods for the normalization approach). This
144 harmonized-resolution analysis (normalized to 500-meter resolution, Table S4) differs from that
145 in Figure S2 and Table S3, which rely instead on each dataset's original resolution and native
146 forest class definitions. Harmonizing the datasets by spatial resolution increased the global
147 congruence only slightly: from 26% to 27% (Table S4, lines 1 and 4). When both normalizing
148 and removing the MODIS dataset with a conflicting forest definition, spatial congruence
149 increased to 45% and 30% for the sparse 10% cover threshold and dense 60% threshold,
150 respectively (Table S4; from 35% and 27% without normalization, respectively, Table S2).
151 Although standardizing resolution increased technical agreement to 45%, a majority of the
152 world's forest area remains subject to incongruent forest data. We further grouped datasets by
153 their forest definition (sparse vs. dense) and recalculated congruence. After normalizing all
154 datasets to a 500-m resolution (10% cover threshold) and using only the six datasets with sparse
155 forest classes, average spatial congruence increased to 47% (from 27%, Table S4: lines 1-3).
156 With a 60% threshold and using only the four datasets with dense forest classes, congruence
157 increased to 42% (Table S4: lines 4-6). These findings illustrate that spatial resolution
158 normalization contributes to improved spatial congruence but explains only part of the spatial
159 disagreement. These patterns also suggest that definitional alignment improves consistency more
160 than resolution normalization alone. Differences in classification methodology, including the
161 choice of algorithm, training data, and the spectral and spatial properties of the input imagery,

162 are also known to affect land cover product accuracy and likely contribute to observed
163 discrepancies in forest representation across GFDs ^{24,28}.

164

165 *Spatial agreement by biome*

166 Spatial agreement on forested areas varied greatly by biome (Fig. 3, Table S5). We found
167 relatively high spatial agreement for the ‘tropical and subtropical moist broadleaf forests’ biome,
168 with 50% of forested area in complete agreement across the eight datasets. In comparison, there
169 was relatively low spatial agreement for the ‘tropical and subtropical dry broadleaf forests’
170 biome, with only 12% of forested area in complete agreement (Fig. 3). We found that the
171 ‘temperate broadleaf and mixed forests,’ ‘temperate conifer forests,’ and ‘boreal forests or taiga’
172 biomes had moderate spatial agreement across the eight datasets, with 33%, 32%, and 23% of
173 area, respectively. The ‘tropical and subtropical coniferous forests’ biome also had low spatial
174 agreement, with 14% of forested area in full agreement. Because of this variance, the total
175 estimated forested land area for each of the 14 biomes varied substantially between GFDs (Table
176 S6).

177

178 *Explaining incongruence across global forest cover datasets*

179 Four main differences explained the (in)congruence between the eight GFDs: (1) spatial
180 resolution, (2) forest definition, (3) classification methodology, and (4) temporal consistency and
181 span.

182 (1) Spatial resolution (defined as the pixel size for classifying land cover) affects estimates
183 because it determines the detail at which land cover patterns can be detected. For
184 example, higher spatial resolution maps could detect distinct forest and agriculture

185 patches in mosaic landscapes. Datasets such as CGLC and JAXA-FNF offer intermediate
186 spatial resolution, losing some of the potential detail of higher resolution data but
187 requiring fewer computational resources to store and process than the higher resolution
188 datasets.

189 (2) Forest definition (defined as the tree canopy cover density and/or height used to define
190 forest land cover classes) affects estimates because it determines which trees are captured
191 in forest estimates. For example, a 10% canopy cover minimum would include sparse
192 savannas whereas a 70% canopy cover minimum would only capture dense forests.
193 ESRI-LC has the most conservative definition of forests (dense clusters of trees), whereas
194 most of the other datasets use a tree canopy cover of 10-15% as the lower cutoff for
195 defining forests. MODIS-IGBP has a conservative definition of forests but also includes
196 savanna classes that capture regions with lower-density tree canopy cover.

197 (3) Classification methodology (defined as the underlying imagery sources and algorithm
198 used to assign land cover labels to pixels) affects estimates because it determines the
199 accuracy of the resulting land cover map. Choices about the sensor, the machine learning
200 algorithm (e.g., random forest, deep learning, decision tree), the class labels used, the
201 quantity and accuracy of the training data^{29,30}, and whether the algorithm is regionally
202 specific (e.g., if different classification algorithms are created for different biomes) all
203 have important implications for land cover maps. Imagery techniques included optical,
204 Synthetic Aperture RADAR (SAR) and light detection and ranging (lidar). For example,
205 ESA-WC and JAXA-FNF incorporate SAR/lidar data along with optical data (e.g.,
206 Sentinel-1 and ALOS PALSAR-2, respectively), whereas most of the other GFD use only
207 optical data (CGLC, ESRI-LC, C3S-LC, and MODIS). GLAD-LCLUC is based on

208 optical Landsat imagery but uses lidar data from GEDI for calibration, enhancing the
209 model's ability to characterize forest structure. Radar imagery allows estimation of
210 vegetation structure and canopy height, especially in regions with frequent cloud cover,
211 while optical imagery is used to measure and classify tree canopy cover and vegetation
212 type. Each type of sensor has strengths and limitations that can influence the resulting
213 dataset's global and regional uncertainty.

214 (4) Temporal consistency (defined as the ability to detect inter-annual changes in forest
215 cover) and temporal span (defined as the available years of data) affect time series
216 analyses. Temporal consistency determines how well the GFD track forest cover loss and
217 gain over time. The data processing methods used to create temporally compatible data
218 affect the uncertainty in detected changes.

219 Across datasets, tradeoffs exist between spatial resolution and temporal span since higher
220 spatial resolutions have only become possible with more recent satellite imagery technology.
221 Longer-term GFD typically had much lower spatial resolution. The ESA-WC and ESRI-LC
222 datasets had the highest spatial resolution (10-meters). However, they were only available for the
223 years 2020-2021 and 2017-2023, respectively. By contrast, ESA-C3S and MODIS Land Cover
224 had the longest temporal coverage (1992-2022 and 2001-2021, respectively), but they had the
225 coarsest spatial resolution (300-meters and 500-meters). GLAD-LCLUC forest extent data were
226 only available for the years 2000 and 2020, but they also provided estimates of total forest cover
227 gain, loss, and disturbance over that period. The two forest cover change datasets (Hansen-GFC
228 and Vancutsem-TMFCC) were both 30-m spatial resolution and multi-decadal.

229

230 *Quantifying the influence of global forest cover dataset selection on sustainability measures*

231 Our global analyses reveal several sources of variation between eight different GFDs,
232 which collectively combine to generate low, and biome-specific, levels of agreement between
233 datasets. Here, we test the practical implications of this (dis)agreement between GFDs on three
234 different case-studies. We selected case study countries across three different continents to
235 demonstrate the differences in GFDs and the implications for countries where there is a
236 concentration of forest-related research^{31,32}. These case studies reveal order-of-magnitude
237 differences in estimates (e.g., a reporting range of between 23.1 million to 252.1 million people
238 living in poverty near forests in India).

239

240 *Above- and below-ground carbon density in forested areas in Kenya*

241 Many authors have used GFDs to estimate carbon storage to identify the effect of climate
242 change policies or conservation (e.g.,^{33,34}). We used the case of Kenya to illustrate how forest
243 dataset selection affects estimates of biomass carbon storage attributed to forests, employing a
244 widely-used above- and below-ground biomass carbon dataset (Fig. S4)³⁵. We selected Kenya
245 due to relatively low spatial GFD agreement (Figs. 1 and S5), the diversity of biomes, and
246 widespread low-density forest systems, allowing us to test the differences between GFD in
247 mapping forest carbon.

248 We overlaid the GFD and biomass carbon data³⁵ to assess relative estimates of carbon in
249 areas classified as forest. We emphasize that this analysis is illustrative and not meant to provide
250 a new estimate of forest biomass carbon. We also note that there is high uncertainty in the
251 carbon density data layer³⁶, which we did not study here.

252 Differences in forest classification had two important implications for estimates of total
253 biomass carbon stored in Kenya's forested areas. First, these differences led to wide variation in

254 the *amount* of carbon, with estimates ranging from 2% (MODIS-IGBP) to 37% (JAXA-FNF) of
255 Kenya's total biomass carbon stored in forests (Table S7). Second, these differences led to
256 variation in the estimated distribution of *where* carbon is stored in forested lands (Fig. 4 and S6).
257 While two datasets may have similar total forest carbon estimates, they were not necessarily
258 distributed equally across space. For example, CGLC and ESRI-LC have similar estimates of
259 total forest carbon in Kenya, but where it is located is dramatically different (Table S7, Fig. S6).

260

261 *Forest-proximate people in poverty in India*

262 Identifying people affected by forest policy decisions is critical for meeting sustainable
263 development goals^{37,38}. We mapped forest-proximate people living in poverty in India, which is
264 the most populated country in the world, where many people rely on forests for their
265 livelihoods³⁹. Forest-proximate people in poverty is used as an indicator of forest dependency,
266 where we defined forest proximity as rural populations living in or within 1 km of a forested
267 area, with poverty status determined using gridded wealth indices calibrated to national poverty
268 rates (Methods). The country has a long history of forest conservation, management, and
269 restoration efforts that are intimately linked with local communities⁴⁰.

270 We found that our national estimates of the number of forest-proximate people living in
271 poverty varied by an order of magnitude among the forest datasets (Table S8). For 2016,
272 estimates varied from 23.1m people (MODIS-IGBP) to 252.1m people (ESA-WC), holding all
273 other variables constant. In contrast to the Kenya case study, the spatial distribution of *where*
274 forest-proximate people were living in poverty was similar when comparing two datasets with
275 similar magnitudes of forest area, such as ESRI-LC and CGLC (Fig. 5) but still drastically
276 different across all eight datasets (Fig. S7). This case study does not imply that one dataset is

277 more accurate or appropriate than the other; rather, it demonstrates how the choice of forest
278 definition and classification system can have large effects on estimates and distribution of forest-
279 proximate populations.

280

281 *Forest habitat for endangered species in Brazil*

282 Forest extent is often used as a proxy for species habitat^{41,42}. We examined how
283 differences in GFD selection may affect biodiversity analyses. We selected Brazil as a case study
284 given its global importance for biodiversity and its well-studied forest cover change dynamics.
285 The white-cheeked spider monkey (*Ateles marginatus*) is an endangered, forest-dwelling species
286 found in the Brazil (in the states of Mato Grosso and Pará). We estimated the forested habitat
287 available within the IUCN defined species range (Table S9) and estimated forest cover change
288 within the region for the period 2016-2021 (Table S10).

289 When considering forest cover *change*, the two forest change datasets (Hansen-GFC and
290 Vancutsem-TMFCC performed dramatically differently, with less than 50% spatial congruence
291 between them (Table S10). Across the six years studied for *A. marginatus*, the two forest cover
292 change- datasets overall exhibited moderate overlap in the area classified as being deforested in
293 each year by both datasets (37% agreement for the period 2016-2021, though this was nearly
294 50% in the single year 2021) (Figs. 6 and S8, Table S10). Importantly, Vancutsem-TMFCC only
295 applies to tropical moist forests, so while the dataset is available across the topical band, it does
296 not capture other forest types.

297

298 **Discussion**

299 We provide systematic evidence that GFD selection can introduce order-of-magnitude
300 uncertainty into monitoring global sustainability challenges. Our results reveal extensive
301 differences in what is classified as “forest” across eight widely used global forest cover datasets
302 (GFDs) and show how dataset choice affects related social and environmental analyses in key
303 sustainability domains. These discrepancies may shape how governments, NGOs, and
304 researchers measure progress toward global climate, biodiversity and development goals. These
305 findings illustrate that millions of people could be overlooked or mistargeted when allocating
306 funding towards forest-based adaptation and livelihood goals and that billions of trees may be
307 overlooked when quantifying the roles of forests and trees towards climate and biodiversity
308 goals. Our findings suggest a need for researchers and decisionmakers who use GFDs to
309 carefully consider the appropriateness of which dataset they select for a given application and/or
310 to use several different GFDs to generate a range of estimates for any given analysis. Based on
311 our review of currently available datasets, we generated a decision tree to help guide user’s
312 dataset selection based on the parameters of their application (Fig. 7).

313 The ten GFDs varied in their spatial resolution, forest definition, classification
314 methodology, and temporal consistency and span. These factors mean that some of these datasets
315 may be less suitable (or indeed, unsuitable) for assessing forest cover and change in some biomes
316 or for some land use types (e.g., fragmented forests or tropical dry forests). Datasets with a
317 higher spatial resolution, such as ESA-WC and GLAD-LCLUC, are more likely to capture
318 smaller features, land cover heterogeneity, and landscape fragmentation. Venter et al. ⁴³ similarly
319 found that ESA-WC was well-suited to detect smaller areas of trees outside of forests, including
320 hedgerows⁴³. However, since some datasets capture tree extent at such a fine spatial resolution,

321 pre-processing steps may be necessary to remove classified tree cover that does not fit the user's
322 desired definition of forests. Reporting often relies on clear definitions of forests, but we show
323 that small definitional differences can translate into large discrepancies in reporting.

324 The 'best fit' dataset for a given application will depend on desired spatial resolution,
325 forest definition, temporal consistency, temporal span, and biome and may change as new
326 datasets and classification algorithms become available. For example, Newton *et al.*³⁸ estimated
327 the number and spatial distribution of forest-proximate people using CGLC data for the primary
328 analyses since it was the best available data at the time of analysis in 2021 (and an improvement
329 on their earlier analysis)^{3,38}. However, as of 2023, ESA-WC and ESRI-LC were available at
330 much higher spatial resolution than CGLC and could now be used to generate improved
331 estimates. Additionally, alternative data products, such as burned area and active fire datasets,
332 have been proposed as potentially useful datasets for tracking forest loss, particularly for regions
333 with deforestation driven by shifting cultivation⁴⁴. Methods have also been proposed to
334 harmonize multiple land cover datasets of different sources and resolutions to improve the
335 accuracy of classification⁴⁵⁻⁴⁷. Such harmonized datasets could be valuable for standardizing
336 monitoring and reporting of climate, biodiversity, and development targets.

337 Our analyses are consonant with recent studies that have also highlighted issues with
338 consistency and accuracy of alternative land cover datasets^{17,18,24,48,49} and the importance of
339 harmonizing forest definitions^{50,51}. We advance previous work by explicitly exploring the
340 implications of forest dataset selection for social-ecological analyses. For example, Sexton *et al.*
341¹⁷ explored the effects of different forest definitions using eight forest cover datasets from around
342 the year 2000 but did not assess how such differences may influence sustainability-related
343 indicators or downstream applications. Our analysis, based on more recent datasets, found

344 similar incongruence among datasets, despite notable improvements in underlying data and
345 processing methods. To illustrate the consequences of these discrepancies, we presented three
346 case studies across different domains: carbon accounting, forest-poverty relationships, and
347 biodiversity habitat. While these examples are not intended to be globally representative, they
348 highlight the types of variability and interpretive challenges that may arise depending on which
349 GFD is selected. Considering the differences that we found in GFD, specific datasets may have
350 been used by researchers in contexts where an alternative dataset might have provided very
351 different insights, and/or where considerable care is needed in interpreting the analyses. While
352 we are not the first to call for such care in using land cover and change datasets (e.g.,^{43,52}), our
353 work provides quantitative examples of how such care is warranted through our case studies.
354 Our aim is to underscore the importance of dataset selection in sustainability applications, not to
355 generalize specific findings across all landscapes.

356 Our analyses lead to three major recommendations. First, we suggest that researchers
357 (and other users of these datasets) carefully review the dataset parameters and the methodology
358 used to produce the datasets when selecting a GFD for a particular purpose⁵³. We provide initial
359 guidance through our decision tree (Fig. 7), which organizes datasets by their spatial resolution,
360 temporal span, and forest definition. However, the optimal GFD is highly dependent on the
361 analytical goal and computational capacity. For instance, moderate resolution datasets (e.g.,
362 CGLC) may be sufficient and more computationally efficient for global environmental (e.g.,
363 forest habitat estimation) or social (e.g., forest-proximate people estimation) analyses, as CGLC
364 (100-meter resolution) performed similarly to the higher resolution datasets like ESA-WC and
365 ESRI-LC (10-meter resolution) in our case studies. While spectral range and resolution are
366 important, the classification quality is also strongly influenced by how time-series imagery and

367 phenological dynamics (e.g., seasonal greenness or land surface phenology) are incorporated into
368 the model. Products that leverage these temporal signals, particularly through multi-season
369 compositing or phenology-informed classifiers, often demonstrate improved accuracy and
370 ecological relevance⁵⁴. National and subnational analyses (e.g., for carbon accounting or species
371 distribution modeling) will generally benefit from higher spatial resolution and time-series-
372 informed forest and tree cover data. Even then, these still need to be used with caution. ESA-WC
373 and ESRI-LC datasets are the highest resolution land cover classification data currently
374 available, but they have important differences in forest definition. We also found that some
375 biomes had more disagreement than others, and caution is especially needed for the tropical and
376 subtropical dry forests biome. Additionally, we note the challenges when interfacing between
377 datasets, such as between the GFDs and the carbon biomass dataset. The underlying spatial
378 resolution and forest definitions of the GFD continue to have big implications when aggregating
379 to a normalized resolution, especially for datasets that do not provide information on the
380 estimated percent tree canopy cover per pixel. For example, it is hard to know what percent of
381 the 300-m biomass carbon pixels is truly covered by trees when normalizing by spatial
382 resolution.

383 Second, we suggest that researchers include sensitivity and uncertainty analyses as a part
384 of studies employing GFD^{38,55}. As illustrated by our case studies, different datasets may generate
385 estimates that can vary by over an order of magnitude. Beyond scrutinizing GFD options and
386 choosing the best available data for their primary analyses, we recommend that researchers test
387 how results vary when using alternative datasets, particularly those with comparable spatial
388 resolution, temporal span, and forest definitions. This approach allows uncertainty to be
389 attributed more directly to classification methodology (e.g., model accuracy, training data) rather

390 than definitional differences alone. Where available, regional or national datasets with different
391 modeling approaches but similar forest definitions can further support sensitivity analyses.
392 However, in many regions such alternatives may not exist. Even in those cases, using multiple
393 global products can still provide a sense of the range of plausible estimates, rather than a single
394 value. To help enable more robust uncertainty analyses, we also recommend that dataset
395 producers provide error bounds or a classification probability maps to indicate pixel-level
396 confidence. Among the ten datasets included in this paper, only CGLC and the MODIS land
397 cover products included such uncertainty indicators.

398 Third, despite improvements in GFD quality, we recommend increased standardization
399 and harmonization of land cover datasets and GFDs through strategic data governance. Given the
400 order-of-magnitude uncertainty introduced by GFD choice, governing bodies (e.g., the UN FAO,
401 UNFCCC, major space agencies, and international earth observation initiatives) could
402 collaboratively generate standardization protocols for forest monitoring. New protocols for
403 reporting both fractional cover (e.g., tree canopy cover percentages) and uncertainty maps are
404 urgently needed. Until GFD producers and key policy data users commit to improved
405 standardization, a fundamental technical choice made in a laboratory will continue to dictate
406 resource allocations and undermine the global community's ability to credibly track progress
407 towards climate and development goals. Given the current lack of data harmonization, we
408 suggest that, where possible, assessments of forest-related policies should use consistent data
409 sources over the analysis period²³. To achieve consistency, researchers can (1) use the same GFD
410 used in the initial policy design, (2) re-generate the baseline assessment using the newly
411 available GFD, or (3) use different datasets for the baseline and endline analysis but assess the
412 resulting potential bias in the estimates and explicitly document the discrepancies. Differences in

413 forest definition and classification methods between datasets, and within the same dataset over
414 time, can lead to biases in impact estimates if the dataset is inconsistent. Additionally, we
415 suggest using care when using forest cover change data. We found that forest cover change
416 datasets (Hansen-GFC and Vancutsem-TMFCC) had considerable disagreement. Accuracy of
417 change detection maps can be affected by the data collection methods, including factors such as
418 seasonality, topography, and shadow presence.

419 One limitation of our approach is driven by the temporal inconsistency across the eight
420 forest cover datasets. CGLC currently was only available through 2019 while ESA-WC was only
421 available for 2020-2021. Additionally, there may be some within-year variability of when the
422 land cover maps were generated based on when the satellite imagery was collected during the
423 year. This likely contributed to some of the differences within our analyses, especially when
424 considering forest cover change. The within-year variability and imagery collection date(s) may
425 be important considerations for research use, where data sources need to be properly
426 harmonized. For the forest cover change comparison, there were important differences in how
427 the Hansen-GFC and Vancutsem-TMFCC datasets tracked change over time. The Hansen-GFC
428 data only records the first year that a pixel is deforested, after which it is removed from future
429 loss classification. Vancutsem-TMFCC, on the other hand, classifies pixels as stable, degraded,
430 deforested, or gain for each year of the dataset, so a pixel can fluctuate through deforestation and
431 regrowth cycles.

432 New datasets continue to be released, creating new possibilities for research using and
433 assessing global forest and tree cover datasets. Some of these new datasets are at unprecedented
434 spatial resolution (e.g., Tolan et al. ⁵⁶), which will further enhance understanding of forest and

435 tree cover dynamics. Future research will need to incorporate these and other new datasets to
436 provide updated guidance on forest cover dataset selection.

437 Additionally, new assessments of accuracy are needed to improve the ability of
438 researchers to use forest cover data appropriately. Validation assessments that are independent
439 (i.e., conducted by a third party, not by dataset developers), based on a common validation
440 dataset designed to be adaptable to different forest definitions, would create a consistent metric
441 with which to compare datasets (e.g., lidar datasets could provide a useful ground truth metric).
442 Biome-specific accuracy assessments would allow researchers to decide which dataset would
443 perform best for an analysis or case study region. Some independent accuracy assessments have
444 been conducted using global ground truth data for some groupings of these datasets^{24,43,57}. For
445 example, both Xu *et al.*²⁴ and Venter *et al.*⁴³ recently compared ESRI-LC, ESA-WC, and
446 Google's Dynamic World (which is a near-real-time, user-generated, 10-m land cover
447 algorithm). While we did not perform accuracy assessments or make use of the uncertainty data
448 associated with several of our included datasets, we echo prior recommendations to carefully
449 evaluate forest cover data in selecting for an application and to conduct accuracy
450 assessments^{26,43}.

451 High quality, regularly updated information on forest cover and forest cover change is
452 critical to inform a wide range of social and environmental sustainability science and policy
453 analyses. Our quantitative comparison of ten widely used public, global forest cover datasets
454 highlights the challenges in accurately mapping forests and forest cover change. Our assessment
455 illustrates how a user's choice of GFD can affect climate, poverty, and biodiversity analyses
456 leading to over an order-of-magnitude difference that can undermine policies aimed to address
457 global agendas. Forests are at the forefront of several key climate and biodiversity agendas,

458 including those of the UNFCCC, the Science Based Targets Network, and the European Union’s
459 Regulation on Deforestation-free Products. Our paper provides insights as to how researchers,
460 policymakers, investors, and forest managers who support or monitor actions to achieve these
461 targets might select appropriate GFD depending on their specific sustainability question of
462 interest.

463

464 **Methods**

465 *Data collection: land cover and forest cover datasets*

466 We identified and compiled globally available datasets to estimate forest cover and forest
467 cover change. We reviewed the properties of each dataset and compared the strengths and
468 weaknesses of each based on published documentation and peer-reviewed analyses. Our review
469 included land/forest cover datasets that: (1) defined at least one forest or tree cover class, (2)
470 included recent years (at least one year between 2018 and 2023), (3) were available globally, and
471 (4) which are publicly available and accessible.

472 The eight land/forest cover datasets we identified were: (1) Copernicus Global Land
473 Cover (CGLC)⁵⁸, (2) GLAD Global Land Cover and Land Use Change (GLAD-LCLUC)⁵⁹, (3)
474 ESA WorldCover (ESA-WC)^{60,61}, (4) ESA Copernicus Climate Change Service Land Cover
475 (ESA-C3S-LC)^{62,63}, (5) ESRI Land Cover (ESRI-LC)⁶⁴, (6) JAXA Forest/Non- Forest (JAXA-
476 FNF)⁶⁵, (7) MODIS Land Cover Type – Annual International Geosphere-Biosphere Programme
477 (IGBP) Classification System (MODIS-IGBP)⁶⁶, and (8) MODIS Land Cover Type – FAO-Land
478 Cover Classification System (MODIS-FAO)⁶⁶. The two forest cover change-specific datasets
479 that we identified were: (1) Vancutsem Tropical Moist Forest Cover Change (Vancutsem-
480 TMFCC)⁶⁷, and (2) Hansen Global Forest Change (Hansen-GFC)⁶⁸. Importantly, Vancutsem-

481 TMFCC applies only to tropical moist forests and does not capture change in other forest types,
482 even within its tropical band coverage. Analysts should take care not to extrapolate its
483 classifications to areas outside its intended biome scope.

484 We present a limited review of 16 other datasets that did not meet our inclusion criteria to
485 provide the reader with historical context and reference material for alternative data sources.

486 These additional resources include GlobeLand30 land cover, Terra MODIS Vegetation
487 Continuous Fields, NASA's GEDI Forest Canopy Height, and the Spatial Database of Planted
488 Trees datasets, as well as 12 historically relevant land/forest cover datasets (Table S1,
489 Supplemental Document S1).

490

491 *Data analysis*

492 We used four approaches to assess agreement between forest cover datasets and to
493 evaluate the implications of the differences among the datasets for social and environmental
494 analyses. First, we mapped the spatial agreement across the eight datasets, quantified pairwise
495 agreement between each dataset, and estimated agreement for each of 14 biomes. Next, we
496 carried out three case study analyses from different world regions to highlight the extent and
497 significance of disagreement among datasets on estimates of (1) above- and below-ground
498 carbon density on forested lands in Kenya, (2) forest-proximate people in poverty for India, and
499 (3) forest habitat for an IUCN red-listed forest-dependent species, the white-cheeked spider
500 monkey, in Brazil.

501 To evaluate spatial agreement between GFDs, we used two complementary methods (Fig.
502 S9):

503 (1) Native-resolution overlay: We overlaid each dataset at its original spatial resolution
504 (e.g., comparing a 500-m dataset directly with a 30-m one), identifying pixels where both
505 datasets classified an area as forest. While this reflects how users might combine off-the-shelf
506 products, it introduces some scale mismatches.

507 (2) Harmonized-resolution comparison: To address these scale mismatches, we also
508 conducted a separate analysis in which all datasets were aggregated to a common 500-meter grid.
509 Fine-resolution datasets were upscaled by calculating the proportion of forest pixels within each
510 coarse 500-m cell from each product's native forest class definition. We then applied consistent
511 forest thresholds or 10% and 60% forest-class coverage to derive binary forest/non-forest maps
512 at 500-m. MODIS datasets were excluded from the alternate threshold analyses when their forest
513 definition did not align with the cutoff.

514 For our analyses, we compared the datasets at their original resolutions and at a
515 normalized spatial resolution (500-m). To harmonize spatial resolution across products, we
516 aggregated each GFD to 500-meter resolution by calculating the percentage of each 500-m cell
517 covered by pixels classified as forest according to the dataset's native classification. We then
518 applied uniform forest cover thresholds (10% and 60%) based on the percent of pixels within the
519 500-m grid that fell into the original forest class(es) to classify the 500-m cells as forested or
520 non-forested. This approach preserves the underlying forest definition of each dataset. No
521 statistical bias correction or regression alignment was performed, as datasets do not measure
522 equivalent biophysical quantities. This process should not be interpreted as statistical
523 normalization of bias across datasets; no regression or calibration was applied, and each
524 product's native classification logic was preserved.

525 We conducted all of our geospatial analyses in Google Earth Engine (GEE)⁶⁹. We
526 generated the maps in ArcGIS Pro using the exported GeoTIFF files from GEE. The global
527 figures are presented at 1000-m spatial resolution, but higher resolution maps are available
528 through GEE (see code availability). The biomass carbon maps published in this paper are
529 presented at 1000-m resolution, the forest-proximate people maps are presented at 100-m
530 resolution, and the forest cover change maps are presented at 30-m resolution. We retained the
531 original spatial resolution for each dataset to maintain the distinct features for each and show
532 how these different data products differ. As a result, a 500-meter forest pixel from one dataset
533 would contain 2,500 10-meter forest and non-forest pixels from another dataset, and the spatial
534 agreement estimate is the area where the datasets agree using the variation down to the 10-meter
535 pixel scale (see Fig. S9 for illustration). For the spatial agreement analysis, we used the full
536 datasets (using all forest or tree cover classes). We used only two of the eight land cover
537 classification systems available for MODIS Land Cover: MODIS-IGBP and MODIS FAO-LLC1
538 (MODIS-FAO). We found that MODIS IGBP, UMD, and LAI had very high similarity and that
539 MODIS FAO-LLC1, FAO-LLC2, APFT, and BCG have very high similarity (Fig. S10).

540

541 *Spatial agreement analysis*

542 We compared the spatial agreement between the eight selected datasets. We overlaid the
543 maps in GEE to determine areas with high and low agreement of forest classification. We
544 tabulated the pairwise agreement between each global dataset to identify the proportion of pixels
545 that each pair of datasets agreed was classified as forest cover. We defined pairwise agreement in
546 two ways:

547 $Pairwise\ Agreement_1 = \frac{Number\ of\ pixels\ both\ i\ and\ j\ define\ as\ forest}{Number\ of\ forest\ pixels\ in\ i + Number\ of\ forest\ pixels\ in\ j}$ (Equation 1)

548 The definition in Equation 1 indicates the proportion of agreement across the entire area
549 defined as forests by either dataset “i” or dataset “j.” The resulting matrix is symmetrical across
550 the diagonal. High agreement using this definition means that both datasets defined forest pixels
551 similarly.

552 $Pairwise\ Agreement_2 = \frac{Number\ of\ pixels\ both\ i\ and\ j\ define\ as\ forest}{Number\ of\ forest\ pixels\ in\ i}$ (Equation 2)

553 The definition in Equation 2 indicates the proportion of agreement across the area defined
554 as forests by only dataset “i.” The resulting matrix is asymmetrical across the diagonal. High
555 agreement using this definition means that dataset “j” captured at least most of the pixels that
556 dataset “i” captured. If in this case, looking across the diagonal there is low agreement, this
557 indicates that dataset “j” defined more pixels as forest than dataset “i.”

558 Additionally, we tabulated the area defined as forests by each of 14 biomes. The biomes
559 are defined by the RESOLVE ecoregions 2017 dataset⁷⁰. We identified datasets for each biome
560 that included significantly more or less forest area based on standard deviation. This allowed us
561 to describe which biomes had high agreement across the datasets, and how the datasets captured
562 forest cover for each biome differently.

563 We do not perform sample-based estimation or formal accuracy assessment. All area and
564 congruence estimates are based on pixel-level comparisons across products using each dataset’s
565 published classification and forest definitions, following a typical user’s experience of applying
566 these products in analyses. This analysis should not be interpreted as statistically representative
567 of forest extent or change.

568

569 *Estimating above- and below-ground carbon density in forested areas in Kenya*

570 To examine the implications of GFD selection on overlaid carbon biomass estimates, we
571 intersected eight forest datasets for 2019–2020 with the 2010 Global Aboveground and
572 Belowground Biomass Carbon Density map³⁵. We chose Kenya for its ecological diversity,
573 policy relevance, and previously observed low GFD congruence. Kenya’s forests are important
574 for livelihoods through timber production, firewood, and non-timber forest products as well as
575 carbon storage⁷¹. Kenya has relatively low forest cover with historically high deforestation rates,
576 but the national government has committed to conserving and restoring its forests through efforts
577 including the African Forest Landscape Restoration Initiative⁷².

578 The biomass carbon data layer was already conditioned on 2010 tree canopy and land
579 cover inputs and therefore partially reflects forest extent. Rather than re-estimating carbon
580 storage for 2020, our goal was to demonstrate how alternative GFDs intersect differently with a
581 fixed carbon layer, simulating a typical user overlay analysis. Since we held the carbon density
582 map constant for our analyses of different GFDs, we considered only relative estimates of
583 biomass carbon rather than generating actual estimates of biomass carbon stored in forests,
584 which would have changed over the decade between 2010 to 2020. Because carbon values were
585 held constant across all GFDs, the results reflect only the effect of forest extent classification
586 differences. We did not attempt to correct for temporal mismatch, biomass uncertainty, or
587 resolution inconsistencies (the biomass carbon dataset is at 300 m resolution). As such, this case
588 study should be interpreted as a demonstration of how GFD choice can influence apparent spatial
589 and quantitative outcomes in carbon accounting, not a formal carbon assessment. Accurate
590 estimation of forest biomass carbon requires harmonizing the scales of the biomass carbon
591 dataset, the ground-truth data used for validation, and the forest extent dataset⁷³. We recognize

592 that this is not a perfect measure of present-day biomass carbon density, but it was sufficient to
593 provide an illustrative analysis to describe the potential impacts of dataset selection on carbon
594 storage estimates in forested areas.

595

596 *Forest-proximate people living in poverty in India*

597 To understand the implications of divergent GFDs for social-economic analysis, we
598 estimated the number of rural forest-proximate people living in poverty in India in the year 2016
599 using each of the eight forest cover datasets (in each case using the closest available year of
600 forest cover data to 2016). For this case study analysis, we transformed the datasets that had a
601 “tree cover” class instead of a forest class (i.e., ESRI-LC and ESA-WC) to use a conservative
602 sparse forest definition of areas of at least 0.5-ha, based on the FAO’s minimum area to define
603 forests. To set the minimum forest size, we removed any tree cover patches that were smaller
604 than 0.5 ha based on square kernel connectedness.

605 We used the methodology developed in Newton *et al.*³⁸ to map the number of forest-
606 proximate people using WorldPop population data (100-m resolution) and each of the forest
607 cover datasets. We defined forest proximity as rural populations living in a forested area or
608 within 1 km of a forest in rural areas, as in Newton *et al.*³⁸. To incorporate the poverty data
609 layer, we used the gridded Relative Wealth Index (RWI) published by Chi *et al.*⁷⁴. The RWI is
610 an asset-based wealth index taken from the Demographic and Health Survey (DHS) Program
611 survey. Chi *et al.*⁷⁴ used machine learning to bring in many other spatial data sources to estimate
612 RWI for the entire country. These estimated RWI data are available nationally in India at a 2.4
613 km spatial resolution. We selected an RWI value such that the number of people in poverty
614 below the RWI threshold matched the national, published multidimensional poverty rate of

615 24.85% for the year of analysis⁷⁵. The RWI threshold that satisfied this criterion was -0.20. This
616 case study is not intended to validate one dataset over another, but rather to assess how
617 differences in forest definitions influence socio-economic indicators when overlaid with
618 population and poverty data.

619

620 *Estimating habitat availability and change for two endangered species in Brazil*

621 We estimated the forested habitat availability for a forest-dwelling, IUCN red-listed
622 endangered species, the white-cheeked spider monkey (*Ateles marginatus*). According to the
623 IUCN Red List species assessment, the primary threat to the white-cheeked spider monkey,
624 extant to Mato Grosso and Pará in Brazil, is the loss of its forest habitat from deforestation due to
625 expanding soy bean farming, cattle ranching, and urbanization⁷⁶.

626 To examine the implications of forest dataset selection on habitat availability and
627 deforestation threat for these species, we overlaid each of the forest cover datasets on the species
628 range polygon shapefile^{77,78} and calculated the area of forest cover defined by each dataset within
629 this polygon. We then used forest cover change datasets for the years 2016-2021 to estimate
630 forest loss within the habitat region. We did not set a constraint on when IUCN conducted the
631 last assessment of the species since we held the species range constant. This may not be a perfect
632 measure of the present-day species range, but it is sufficient to provide an illustrative analysis to
633 describe the estimates of forested habitat areas.

634 For forest cover change estimation, we used the two land cover change datasets (Hansen-
635 GFC and Vancutsem-TMFCC) as the primary focus of the analysis. We do not report results
636 using the panel of the annual land cover datasets (taking the difference between the raster maps
637 across years) since this approach does not use rigorous change detection algorithms and can lead

638 to false positive or negative changes. For the Hansen-GFC dataset, we isolated loss data for each
639 year. For the Vancutsem-TMFCC dataset, we followed the methods presented by European
640 Commission (2021) to create maps for forest cover loss (deforestation only and deforestation
641 plus degradation) and gain for each year⁷⁹.

642

643 **Resource availability**

644 *Lead contact*

645 Further information and requests for resources should be directed to Sarah Castle

646 (castle3@wisc.edu).

647 *Materials availability*

648 This study did not generate new unique materials.

649 *Data and code availability*

650 **Data:** All datasets used in this study were derived from published sources cited in the
651 Methods section. The following datasets are available through the Google Earth Engine (GEE)
652 Data Catalog (Accessed: 15 December 2023):

- 653 • Copernicus Global Land Cover (CGLC) ([https://developers.google.com/earth-](https://developers.google.com/earth-engine/datasets/catalog/COPERNICUS_Landcover_100m_Proba-V-C3_Global)
654 [engine/datasets/catalog/COPERNICUS_Landcover_100m_Proba-V-C3_Global](https://developers.google.com/earth-engine/datasets/catalog/COPERNICUS_Landcover_100m_Proba-V-C3_Global))
- 655 • ESA WorldCover (ESA-WC) ([https://developers.google.com/earth-](https://developers.google.com/earth-engine/datasets/catalog/ESA_WorldCover_v100)
656 [engine/datasets/catalog/ESA_WorldCover_v100](https://developers.google.com/earth-engine/datasets/catalog/ESA_WorldCover_v100) and
657 https://developers.google.com/earth-engine/datasets/catalog/ESA_WorldCover_v200)
- 658 • JAXA Forest/Non- Forest (JAXA-FNF) ([https://developers.google.com/earth-](https://developers.google.com/earth-engine/datasets/catalog/JAXA_ALOS_PALSAR_YEARLY_FNF4)
659 [engine/datasets/catalog/JAXA_ALOS_PALSAR_YEARLY_FNF4](https://developers.google.com/earth-engine/datasets/catalog/JAXA_ALOS_PALSAR_YEARLY_FNF4))

- 660 • MODIS Land Cover Type (MODIS-LC) ([https://developers.google.com/earth-](https://developers.google.com/earth-engine/datasets/catalog/MODIS_061_MCD12Q1)
661 [engine/datasets/catalog/MODIS_061_MCD12Q1](https://developers.google.com/earth-engine/datasets/catalog/MODIS_061_MCD12Q1))
- 662 • Hansen Global Forest Change (Hansen-GFC) ([https://developers.google.com/earth-](https://developers.google.com/earth-engine/datasets/catalog/UMD_hansen_global_forest_change_2022_v1_10)
663 [engine/datasets/catalog/UMD_hansen_global_forest_change_2022_v1_10](https://developers.google.com/earth-engine/datasets/catalog/UMD_hansen_global_forest_change_2022_v1_10))
- 664 • WorldPop for administrative boundaries and gridded population density data
665 (https://developers.google.com/earth-engine/datasets/catalog/WorldPop_GP_100m_pop).
- 666 • RESOLVE Ecoregions 2017 for biome limits ([https://developers.google.com/earth-](https://developers.google.com/earth-engine/datasets/catalog/RESOLVE_ECOREGIONS_2017)
667 [engine/datasets/catalog/RESOLVE_ECOREGIONS_2017](https://developers.google.com/earth-engine/datasets/catalog/RESOLVE_ECOREGIONS_2017))

668 ESA Copernicus Climate Change Service Land Cover (ESA-C3S-LC) was available for
669 download from <https://cds.climate.copernicus.eu/cdsapp#!/dataset/satellite-land-cover>
670 (Accessed: 15 December 2023). ESRI Land Cover (ESRI-LC) was available on GEE using the
671 code available from <https://gee-community-catalog.org/projects/S2TSLULC/> (Accessed: 15
672 December 2023). GLAD Global Land Cover and Land Use Change (GLAD-LCLUC) was
673 available on GEE using the code available from <https://glad.umd.edu/dataset/GLCLUC2020>
674 (Accessed: 15 December 2023). Vancutsem Tropical Moist Forest Cover Change (Vancutsem-
675 TMFCC) was available on GEE using the code available from
676 <https://forobs.jrc.ec.europa.eu/TMF> (Accessed: 15 December 2023).

677 The Spawn *et al.*³⁵ aboveground and belowground biomass carbon density data is
678 available to download from
679 https://daac.ornl.gov/VEGETATION/guides/Global_Maps_C_Density_2010.html (Accessed: 15
680 December 2023). The species habitat ranges were obtained for the IUCN Red List database
681 (available for download from: <https://www.iucnredlist.org> with valid request; Accessed: 15

682 December 2023). Gridded relative wealth index data from Chi *et al.* ⁷⁴ were downloaded from
683 <https://data.humdata.org/dataset/relative-wealth-index> (Accessed: 15 December 2023).

684 High resolution images for figures 1, 4, 5, and 6 are available on figshare
685 dx.doi.org/10.6084/m9.figshare.24898275.

686
687 **Code:** The Google Earth Engine codes for data processing and analyses are openly
688 available through GitHub at: <https://github.com/saraheb3/forestdatasets/>. Datasets without
689 sharing restrictions (e.g., those available in the Google Earth Engine data catalog) are directly
690 accessible in the published code. Datasets with sharing restrictions (e.g., IUCN red list species
691 habitat layers) are not shared as assets, but users may download the latest IUCN red list species
692 habitat layers and import them into the code to run their own analyses.

693

694 **Supplemental information**

695 Document S1: Supplemental documentation of key aspects of the global forest (land) cover and
696 change datasets.

697 Figures S1-S10. Tables S1-S10. Supplemental references.

698 **Acknowledgments**

699 We thank Rayna Benzeev, Polyanna Bispo, Christopher Castle, Mohammad Farrae,
700 Andrew Kinzer, and Sam Stickley for providing valuable feedback that helped improve this
701 paper. Funding from Notre Dame Research and the Pulte Institute for Global Development
702 through University of Notre Dame Poverty Initiative is gratefully acknowledged. S.E.C. was
703 funded by a University of Illinois Graduate College Dissertation Completion Fellowship. J.A.O.
704 was funded by a UKRI Frontier Research Grant (No. EP/X023222/1), selected by the European

705 Research Council. We are grateful to the Editor and four anonymous reviewers for comments
706 that enabled us to substantially improve this article.

707

708 **Author contributions**

709 Conceptualization: S.E.C, P.N., J.A.O., and D.C.M.; Methodology: S.E.C, P.N., J.A.O., K.B.,
710 and D.C.M.; Formal Analysis: S.E.C.; Writing – Original Draft: S.E.C.; Writing – Review &
711 Editing: S.E.C, P.N., J.A.O., K.B., and D.C.M.; Visualization: S.E.C. and J.A.O.; Supervision:
712 D.C.M.; Funding Acquisition: S.E.C, J.A.O., and D.C.M.

713

714 **Declaration of interests**

715 The authors declare no competing interests.

716

717 **Declaration of Generative AI and AI-assisted technologies in the writing process**

718 During the preparation of this work the authors used Microsoft Copilot with a detailed set of
719 prompts to generate the initial draft of the graphical abstract, and we sparingly used Gemini to
720 edit language for clarity and conciseness during the manuscript review process. The original
721 submission was written with no use of AI. After using this tool, the authors carefully reviewed
722 and edited the content and takes full responsibility for the content of the publication.

723

724 **References**

- 725 1. Harris, N.L., Gibbs, D.A., Baccini, A., Birdsey, R.A., de Bruin, S., Farina, M., Fatoyinbo, L., Hansen,
726 M.C., Herold, M., Houghton, R.A., et al. (2021). Global maps of twenty-first century forest
727 carbon fluxes. *Nature Climate Change* *11*, 234-240. 10.1038/s41558-020-00976-6.
- 728 2. FAO and UNEP (2020). *The State of the World's Forests 2020. Forests, biodiversity and people.*
729 FAO.
- 730 3. Newton, P., Kinzer, A.T., Miller, D.C., Oldekop, J.A., and Agrawal, A. (2020). The number and
731 spatial distribution of forest-proximate people globally. *One Earth* *3*, 363-370.
732 <https://doi.org/10.1016/j.oneear.2020.08.016>.
- 733 4. Miller, D.C., Mansourian, S., and Wildburger, C. (2020). *Forests, Trees and the Eradication of*
734 *Poverty: Potential and Limitations. A Global Assessment Report (IUFRO World Series).*
- 735 5. FAO (2022). *The State of the World's Forests 2022: Forest pathways for green recovery and*
736 *building inclusive, resilient and sustainable economies.* FAO.
- 737 6. Börner, J., Schulz, D., Wunder, S., and Pfaff, A. (2020). The Effectiveness of Forest Conservation
738 Policies and Programs. *Annual Review of Resource Economics* *12*, 45-64. 10.1146/annurev-
739 resource-110119-025703.
- 740 7. Ordóñez, P.J., Baylis, K., and Ramírez, M.I. (2023). Land cover change effects from community
741 forest management in Michoacán, Mexico. *Environmental Research Letters* *18*, 065008.
742 10.1088/1748-9326/accdef.
- 743 8. West, T.A.P., Wunder, S., Sills, E.O., Börner, J., Rifai, S.W., Neidermeier, A.N., Frey, G.P., and
744 Kontoleon, A. (2023). Action needed to make carbon offsets from forest conservation work for
745 climate change mitigation. *Science* *381*, 873-877. 10.1126/science.ade3535.
- 746 9. Souza, C.M., Z. Shimbo, J., Rosa, M.R., Parente, L.L., A. Alencar, A., Rudorff, B.F.T., Hasenack, H.,
747 Matsumoto, M., G. Ferreira, L., Souza-Filho, P.W.M., et al. (2020). Reconstructing Three Decades
748 of Land Use and Land Cover Changes in Brazilian Biomes with Landsat Archive and Earth Engine.
749 *Remote Sensing* *12*, 2735.
- 750 10. Canada Centre for Remote Sensing (CCRS)/Canada Centre for Mapping and Earth Observation
751 (CCMEO), Natural Resources Canada (NRCan), Comisión Nacional para el Conocimiento y Uso de
752 la Biodiversidad (CONABIO), Comisión Nacional Forestal (CONAFOR), Instituto Nacional de
753 Estadística y Geografía (INEGI), and (USGS), U.S.G.S. (2023). 2020 Land Cover of North America
754 at 30 meters. Version 1.0 <http://www.cec.org/nalcms>.
- 755 11. Dewitz, J. (2021). National Land Cover Database (NLCD) 2019 Products (ver. 3.0, February 2024)
756 [Data set]. U.S. Geological Survey. <https://doi.org/10.5066/P9KZCM54>.
- 757 12. Büttner, G. (2014). CORINE land cover and land cover change products. In *Land use and land*
758 *cover mapping in Europe: practices & trends*, (Springer), pp. 55-74.
- 759 13. d'Andrimont, R., Yordanov, M., Martinez-Sanchez, L., Haub, P., Buck, O., Haub, C., Eiselt, B., and
760 van der Velde, M. (2022). LUCAS cover photos 2006–2018 over the EU: 874 646 spatially
761 distributed geo-tagged close-up photos with land cover and plant species label. *Earth Syst. Sci.*
762 *Data* *14*, 4463-4472. 10.5194/essd-14-4463-2022.
- 763 14. Yang, J., and Huang, X. (2023). The 30 m annual land cover datasets and its dynamics in China
764 from 1985 to 2022. *Earth System Science Data*. 10.5281/zenodo.8176941.
- 765 15. Li, Z., He, W., Cheng, M., Hu, J., Yang, G., and Zhang, H. (2023). SinoLC-1: the first 1 m
766 resolution national-scale land-cover map of China created with a deep learning framework and
767 open-access data. *Earth Syst. Sci. Data* *15*, 4749-4780. 10.5194/essd-15-4749-2023.

- 768 16. Fritz, S., and See, L. (2008). Identifying and quantifying uncertainty and spatial disagreement in
769 the comparison of Global Land Cover for different applications. *Global Change Biology* 14, 1057-
770 1075. <https://doi.org/10.1111/j.1365-2486.2007.01519.x>.
- 771 17. Sexton, J.O., Noojipady, P., Song, X.-P., Feng, M., Song, D.-X., Kim, D.-H., Anand, A., Huang, C.,
772 Channan, S., Pimm, S.L., and Townshend, J.R. (2016). Conservation policy and the measurement
773 of forests. *Nature Climate Change* 6, 192-196. 10.1038/nclimate2816.
- 774 18. Pérez-Hoyos, A., Rembold, F., Kerdiles, H., and Gallego, J. (2017). Comparison of Global Land
775 Cover Datasets for Cropland Monitoring. *Remote Sensing* 9, 1118.
776 <https://doi.org/10.3390/rs9111118>.
- 777 19. Chen, H., Zeng, Z., Wu, J., Peng, L., Lakshmi, V., Yang, H., and Liu, J. (2020). Large Uncertainty on
778 Forest Area Change in the Early 21st Century among Widely Used Global Land Cover Datasets.
779 *Remote Sensing* 12, 3502.
- 780 20. Li, Y., Sulla-Menashe, D., Motesharrei, S., Song, X.-P., Kalnay, E., Ying, Q., Li, S., and Ma, Z.
781 (2017). Inconsistent estimates of forest cover change in China between 2000 and 2013 from
782 multiple datasets: differences in parameters, spatial resolution, and definitions. *Scientific*
783 *Reports* 7, 8748. 10.1038/s41598-017-07732-5.
- 784 21. Garcia, A., and Heilmayr, R. (2022). Conservation impact evaluation using remotely sensed data.
785 <http://dx.doi.org/10.2139/ssrn.4179782>
- 786 22. Donaldson, D., and Storeygard, A. (2016). The View from Above: Applications of Satellite Data in
787 Economics. *Journal of Economic Perspectives* 30, 171-198. 10.1257/jep.30.4.171.
- 788 23. Jain, M. (2020). The Benefits and Pitfalls of Using Satellite Data for Causal Inference. *Review of*
789 *Environmental Economics and Policy* 14, 157-169. 10.1093/reep/rez023.
- 790 24. Xu, P., Tsendbazar, N.-E., Herold, M., de Bruin, S., Koopmans, M., Birch, T., Carter, S., Fritz, S.,
791 Lesiv, M., Mazur, E., et al. (2024). Comparative validation of recent 10 m-resolution global land
792 cover maps. *Remote Sensing of Environment* 311, 114316.
793 <https://doi.org/10.1016/j.rse.2024.114316>.
- 794 25. FAO (2023). *Global Forest Resources Assessment 2025: Terms and Definitions*. Food and
795 Agriculture Organization of the United Nations.
- 796 26. Olofsson, P., Foody, G.M., Herold, M., Stehman, S.V., Woodcock, C.E., and Wulder, M.A. (2014).
797 Good practices for estimating area and assessing accuracy of land change. *Remote Sensing of*
798 *Environment* 148, 42-57. <https://doi.org/10.1016/j.rse.2014.02.015>.
- 799 27. Jonckheere, I., Hamilton, R., Michel, J.M., and Donegan, E., eds. (2024). Good practices in
800 sample-based area estimation. White paper. (FAO). <https://doi.org/10.4060/cc9276en>.
- 801 28. Basheer, S., Wang, X., Farooque, A.A., Nawaz, R.A., Liu, K., Adekanmbi, T., and Liu, S. (2022).
802 Comparison of Land Use Land Cover Classifiers Using Different Satellite Imagery and Machine
803 Learning Techniques. *Remote Sensing* 14, 4978.
- 804 29. Stanimirova, R., Tarrío, K., Turlej, K., McAvoy, K., Stonebrook, S., Hu, K.-T., Arévalo, P., Bullock,
805 E.L., Zhang, Y., Woodcock, C.E., et al. (2023). A global land cover training dataset from 1984 to
806 2020. *Scientific Data* 10, 879. 10.1038/s41597-023-02798-5.
- 807 30. White, J.C., Coops, N.C., Wulder, M.A., Vastaranta, M., Hilker, T., and Tompalski, P. (2016).
808 Remote Sensing Technologies for Enhancing Forest Inventories: A Review. *Canadian Journal of*
809 *Remote Sensing* 42, 619-641. 10.1080/07038992.2016.1207484.
- 810 31. Cheng, S.H., MacLeod, K., Ahlroth, S., Onder, S., Perge, E., Shyamsundar, P., Rana, P., Garside, R.,
811 Kristjanson, P., McKinnon, M.C., and Miller, D.C. (2019). A systematic map of evidence on the
812 contribution of forests to poverty alleviation. *Environmental Evidence* 8, 3. 10.1186/s13750-019-
813 0148-4.

- 814 32. Miller, D.C., Ordoñez, P.J., Brown, S.E., Forrest, S., Nava, N.J., Hughes, K., and Baylis, K. (2020).
815 The impacts of agroforestry on agricultural productivity, ecosystem services, and human well-
816 being in low-and middle-income countries: An evidence and gap map. *Campbell Systematic*
817 *Reviews* 16, e1066. [10.1002/cl2.1066](https://doi.org/10.1002/cl2.1066).
- 818 33. Noon, M.L., Goldstein, A., Ledezma, J.C., Roehrdanz, P.R., Cook-Patton, S.C., Spawn-Lee, S.A.,
819 Wright, T.M., Gonzalez-Roglich, M., Hole, D.G., Rockström, J., and Turner, W.R. (2022). Mapping
820 the irrecoverable carbon in Earth's ecosystems. *Nature Sustainability* 5, 37-46. [10.1038/s41893-](https://doi.org/10.1038/s41893-021-00803-6)
821 [021-00803-6](https://doi.org/10.1038/s41893-021-00803-6).
- 822 34. Santoro, M., Cartus, O., Carvalhais, N., Rozendaal, D.M.A., Avitabile, V., Araza, A., de Bruin, S.,
823 Herold, M., Quegan, S., Rodríguez-Veiga, P., et al. (2021). The global forest above-ground
824 biomass pool for 2010 estimated from high-resolution satellite observations. *Earth Syst. Sci.*
825 *Data* 13, 3927-3950. [10.5194/essd-13-3927-2021](https://doi.org/10.5194/essd-13-3927-2021).
- 826 35. Spawn, S.A., Sullivan, C.C., Lark, T.J., and Gibbs, H.K. (2020). Harmonized global maps of above
827 and belowground biomass carbon density in the year 2010. *Scientific Data* 7, 112.
828 [10.1038/s41597-020-0444-4](https://doi.org/10.1038/s41597-020-0444-4).
- 829 36. Araza, A., de Bruin, S., Herold, M., Quegan, S., Labriere, N., Rodriguez-Veiga, P., Avitabile, V.,
830 Santoro, M., Mitchard, E.T.A., Ryan, C.M., et al. (2022). A comprehensive framework for
831 assessing the accuracy and uncertainty of global above-ground biomass maps. *Remote Sensing*
832 *of Environment* 272, 112917. <https://doi.org/10.1016/j.rse.2022.112917>.
- 833 37. Erbaugh, J.T., Pradhan, N., Adams, J., Oldekop, J.A., Agrawal, A., Brockington, D., Pritchard, R.,
834 and Chhatre, A. (2020). Global forest restoration and the importance of prioritizing local
835 communities. *Nature Ecology & Evolution*. [10.1038/s41559-020-01282-2](https://doi.org/10.1038/s41559-020-01282-2).
- 836 38. Newton, P., Castle, S.E., Kinzer, A.T., Miller, D.C., Oldekop, J.A., Linhares-Juvenal, T., Madrid, M.,
837 Pina, L., and de Lamo Rodriguez, J. (2022). The number of forest- and tree-proximate people: a
838 new methodology and global estimates. *FAO*.
- 839 39. Damania, R., Joshi, A., and Russ, J. (2020). India's forests – Stepping stone or millstone for the
840 poor? *World Development* 125, 104451. <https://doi.org/10.1016/j.worlddev.2018.11.007>.
- 841 40. Agrawal, A. (2005). *Environmentality: Technologies of Government and the Making of Subjects*
842 (Duke University Press). doi:10.1515/9780822386421.
- 843 41. Hill, S.L.L., Arnell, A., Maney, C., Butchart, S.H.M., Hilton-Taylor, C., Ciciarelli, C., Davis, C.,
844 Dinerstein, E., Purvis, A., and Burgess, N.D. (2019). Measuring Forest Biodiversity Status and
845 Changes Globally. *Frontiers in Forests and Global Change* 2. [10.3389/ffgc.2019.00070](https://doi.org/10.3389/ffgc.2019.00070).
- 846 42. Brooks, T.M., Pimm, S.L., Akçakaya, H.R., Buchanan, G.M., Butchart, S.H.M., Foden, W., Hilton-
847 Taylor, C., Hoffmann, M., Jenkins, C.N., Joppa, L., et al. (2019). Measuring Terrestrial Area of
848 Habitat (AOH) and Its Utility for the IUCN Red List. *Trends in Ecology & Evolution* 34, 977-986.
849 [10.1016/j.tree.2019.06.009](https://doi.org/10.1016/j.tree.2019.06.009).
- 850 43. Venter, Z.S., Barton, D.N., Chakraborty, T., Simensen, T., and Singh, G. (2022). Global 10 m Land
851 Use Land Cover Datasets: A Comparison of Dynamic World, World Cover and Esri Land Cover.
852 *Remote Sensing* 14, 4101. <https://doi.org/10.3390/rs14164101>.
- 853 44. Papunen, S., and Eklund, J. (2024). Comparing the performance of three satellite-based data
854 products for assessing protected area effectiveness. *Global Ecology and Conservation* 52,
855 e02954. <https://doi.org/10.1016/j.gecco.2024.e02954>.
- 856 45. Song, X.-P., Huang, C., Feng, M., Sexton, J.O., Channan, S., and Townshend, J.R. (2014).
857 Integrating global land cover products for improved forest cover characterization: an application
858 in North America. *International Journal of Digital Earth* 7, 709-724.
859 [10.1080/17538947.2013.856959](https://doi.org/10.1080/17538947.2013.856959).

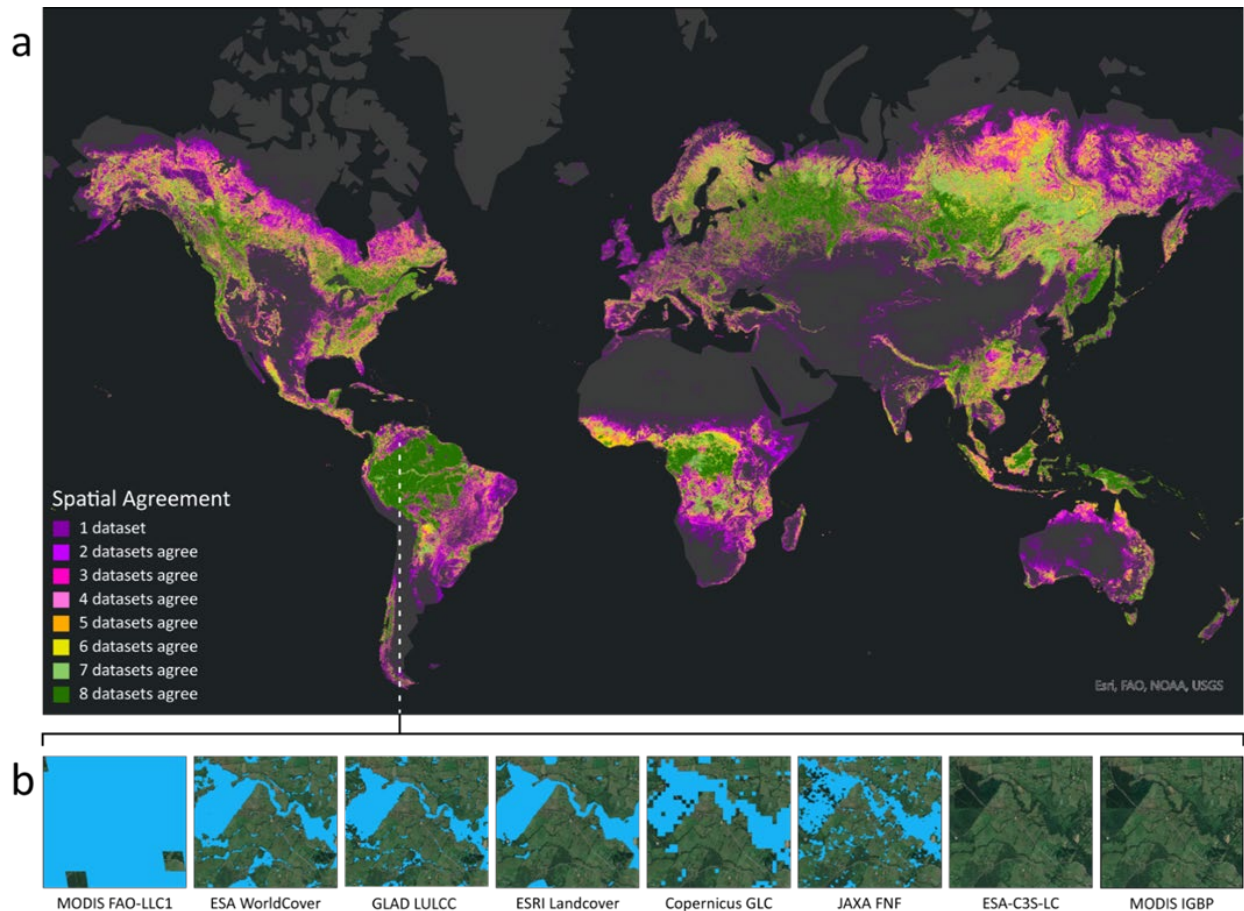
- 860 46. Schepaschenko, D., See, L., Lesiv, M., McCallum, I., Fritz, S., Salk, C., Moltchanova, E., Perger, C.,
861 Shchepashchenko, M., Shvidenko, A., et al. (2015). Development of a global hybrid forest mask
862 through the synergy of remote sensing, crowdsourcing and FAO statistics. *Remote Sensing of*
863 *Environment* 162, 208-220. <https://doi.org/10.1016/j.rse.2015.02.011>.
- 864 47. Vancutsem, C., Marinho, E., Kayitakire, F., See, L., and Fritz, S. (2013). Harmonizing and
865 Combining Existing Land Cover/Land Use Datasets for Cropland Area Monitoring at the African
866 Continental Scale. *Remote Sensing* 5, 19-41. <https://doi.org/10.3390/rs5010019>.
- 867 48. Pendrill, F., Gardner, T.A., Meyfroidt, P., Persson, U.M., Adams, J., Azevedo, T., Bastos Lima,
868 M.G., Baumann, M., Curtis, P.G., De Sy, V., et al. (2022). Disentangling the numbers behind
869 agriculture-driven tropical deforestation. *Science* 377, eabm9267. 10.1126/science.abm9267.
- 870 49. Pérez-Hoyos, A., García-Haro, F.J., and San-Miguel-Ayanz, J. (2012). Conventional and fuzzy
871 comparisons of large scale land cover products: Application to CORINE, GLC2000, MODIS and
872 GlobCover in Europe. *ISPRS Journal of Photogrammetry and Remote Sensing* 74, 185-201.
873 <https://doi.org/10.1016/j.isprsjprs.2012.09.006>.
- 874 50. Fernández-Montes de Oca, A.I., Gallardo-Cruz, J.A., Ghilardi, A., Kauffer, E., Solórzano, J.V., and
875 Sánchez-Cordero, V. (2021). An integrated framework for harmonizing definitions of
876 deforestation. *Environmental Science & Policy* 115, 71-78.
877 <https://doi.org/10.1016/j.envsci.2020.10.007>.
- 878 51. Chazdon, R.L., Brancalion, P.H.S., Laestadius, L., Bennett-Curry, A., Buckingham, K., Kumar, C.,
879 Moll-Rocek, J., Vieira, I.C.G., and Wilson, S.J. (2016). When is a forest a forest? Forest concepts
880 and definitions in the era of forest and landscape restoration. *Ambio* 45, 538-550.
881 10.1007/s13280-016-0772-y.
- 882 52. Neuendorf, F., Thiele, J., Albert, C., and von Haaren, C. (2021). Uncertainties in land use data
883 may have substantial effects on environmental planning recommendations: A plea for careful
884 consideration. *PLOS ONE* 16, e0260302. 10.1371/journal.pone.0260302.
- 885 53. Verburg, P.H., Neumann, K., and Nol, L. (2011). Challenges in using land use and land cover data
886 for global change studies. *Global change biology* 17, 974-989. <https://doi.org/10.1111/j.1365-2486.2010.02307.x>.
- 888 54. Gómez, C., White, J.C., and Wulder, M.A. (2016). Optical remotely sensed time series data for
889 land cover classification: A review. *ISPRS Journal of Photogrammetry and Remote Sensing* 116,
890 55-72. <https://doi.org/10.1016/j.isprsjprs.2016.03.008>.
- 891 55. Pessôa, A.C.M., Anderson, L.O., Carvalho, N.S., Campanharo, W.A., Junior, C.H.L.S., Rosan, T.M.,
892 Reis, J.B.C., Pereira, F.R.S., Assis, M., Jacon, A.D., et al. (2020). Intercomparison of Burned Area
893 Products and Its Implication for Carbon Emission Estimations in the Amazon. *Remote Sensing* 12,
894 3864. <https://doi.org/10.3390/rs12233864>.
- 895 56. Tolan, J., Yang, H.-I., Nosarzewski, B., Couairon, G., Vo, H.V., Brandt, J., Spore, J., Majumdar, S.,
896 Haziza, D., Vamaraju, J., et al. (2024). Very high resolution canopy height maps from RGB
897 imagery using self-supervised vision transformer and convolutional decoder trained on aerial
898 lidar. *Remote Sensing of Environment* 300, 113888. <https://doi.org/10.1016/j.rse.2023.113888>.
- 899 57. Song, X.P., Huang, C., Sexton, J.O., Feng, M., Narasimhan, R., Channan, S., and Townshend, J.R.
900 (2011). An assessment of global forest cover maps using regional higher-resolution reference
901 data sets. 24-29 July 2011. pp. 752-755.
- 902 58. Buchhorn, M., Lesiv, M., Tsendbazar, N.-E., Herold, M., Bertels, L., and Smets, B. (2020).
903 Copernicus global land cover layers—collection 2. *Remote Sensing* 12, 1044.
904 <https://doi.org/10.3390/rs12061044>.

- 905 59. Potapov, P., Hansen, M.C., Pickens, A., Hernandez-Serna, A., Tyukavina, A., Turubanova, S.,
906 Zalles, V., Li, X., Khan, A., Stolle, F., et al. (2022). The Global 2000-2020 Land Cover and Land Use
907 Change Dataset Derived From the Landsat Archive: First Results. *Frontiers in Remote Sensing* 3.
908 10.3389/frsen.2022.856903.
- 909 60. Zanaga, D., Van De Kerchove, R., De Keersmaecker, W., Souverijns, N., Brockmann, C., Quast, R.,
910 Wevers, J., Grosu, A., Paccini, A., Vergnaud, S., et al. (2021). *ESA WorldCover 10 m 2020 v100*.
- 911 61. Zanaga, D., Van De Kerchove, R., Daems, D., De Keersmaecker, W., Brockmann, C., Kirches, G.,
912 Wevers, J., Cartus, O., Santoro, M., Fritz, S., et al. (2022). *ESA WorldCover 10 m 2021 v200*.
913 <https://doi.org/10.5281/zenodo.7254221>.
- 914 62. ESA (2017). *Land Cover CCI Product User Guide Version 2*.
- 915 63. Defourny, P., Lamarche, C., Flasse, C., Kirches, G., Böttcher, M., and Brockmann, C. (2019). *C3S -*
916 *Product User Guide and Specification ICDR Land Cover 2016 to 2018, v1.2*.
- 917 64. Karra, K., Kontgis, C., Statman-Weil, Z., Mazzariello, J.C., Mathis, M., and Brumby, S.P. (2021).
918 Global land use/land cover with Sentinel 2 and deep learning. *2021 IEEE International*
919 *Geoscience and Remote Sensing Symposium IGARSS*, 4704-4707.
- 920 65. Shimada, M., Itoh, T., Motooka, T., Watanabe, M., Shiraishi, T., Thapa, R., and Lucas, R. (2014).
921 New global forest/non-forest maps from ALOS PALSAR data (2007–2010). *Remote Sensing of*
922 *Environment* 155, 13-31. <https://doi.org/10.1016/j.rse.2014.04.014>.
- 923 66. Friedl, M., and Sulla-Menashe, D. (2015). MCD12Q1 MODIS/Terra+ aqua land cover type yearly
924 L3 global 500m SIN grid V006 [data set]. *NASA EOSDIS Land Processes DAAC* 10, 200.
- 925 67. Vancutsem, C., Achard, F., Pekel, J.-F., Vieilledent, G., Carboni, S., Simonetti, D., Gallego, J.,
926 Aragão, L.E.O.C., and Nasi, R. (2021). Long-term (1990-2019) monitoring of forest cover changes
927 in the humid tropics. *Science Advances* 7, eabe1603. 10.1126/sciadv.abe1603.
- 928 68. Hansen, M.C., Potapov, P.V., Moore, R., Hancher, M., Turubanova, S.A., Tyukavina, A., Thau, D.,
929 Stehman, S., Goetz, S.J., and Loveland, T.R. (2013). High-resolution global maps of 21st-century
930 forest cover change. *science* 342, 850-853.
- 931 69. Gorelick, N., Hancher, M., Dixon, M., Ilyushchenko, S., Thau, D., and Moore, R. (2017). Google
932 Earth Engine: Planetary-scale geospatial analysis for everyone. *Remote Sensing of Environment*
933 202, 18-27. <https://doi.org/10.1016/j.rse.2017.06.031>.
- 934 70. Dinerstein, E., Olson, D., Joshi, A., Vynne, C., Burgess, N.D., Wikramanayake, E., Hahn, N.,
935 Palminteri, S., Hedao, P., Noss, R., et al. (2017). An Ecoregion-Based Approach to Protecting Half
936 the Terrestrial Realm. *BioScience* 67, 534-545. 10.1093/biosci/bix014.
- 937 71. Rodríguez-Veiga, P., Carreiras, J., Smallman, T.L., Exbrayat, J.-F., Ndambiri, J., Mutwiri, F.,
938 Nyasaka, D., Quegan, S., Williams, M., and Balzter, H. (2020). Carbon Stocks and Fluxes in
939 Kenyan Forests and Wooded Grasslands Derived from Earth Observation and Model-Data
940 Fusion. *Remote Sensing* 12, 2380. <https://doi.org/10.3390/rs12152380>.
- 941 72. Gichu, A., Kahuri, S., Minnick, A., Landsberg, F., Ndunda, P., Koome, N., Neema, N., and Oyuke, J.
942 (2022). Technical Report on the National Assessment of Forest and Landscape Restoration
943 Opportunities in Kenya 2016. Kenya Ministry of Environment and Natural Resources, Kenya
944 Forest Service.
- 945 73. Duncanson, L., Hunka, N., Jucker, T., Armston, J., Harris, N., Fatoyinbo, L., Williams, C.A., Atkins,
946 J.W., Raczka, B., Serbin, S., et al. (2025). Spatial resolution for forest carbon maps. *Science* 387,
947 370-371. doi:10.1126/science.adt6811.
- 948 74. Chi, G., Fang, H., Chatterjee, S., and Blumenstock, J.E. (2022). Microestimates of wealth for all
949 low- and middle-income countries. *Proceedings of the National Academy of Sciences* 119,
950 e2113658119. doi:10.1073/pnas.2113658119.

- 951 75. OPHI, UNDP, and Aayog, N. (2023). National Multidimensional Poverty Index (MPI): A Progress
952 Review 2023
- 953 76. Ravetta, A.L., Buss, G., and Mittermeier, R.A. (2021). *Ateles marginatus* (amended version of
954 2019 assessment). The IUCN Red List of Threatened Species 2021: e.T2282A191689524.
- 955 77. IUCN (International Union for Conservation of Nature) (2008). *Ateles marginatus*. The IUCN Red
956 List of Threatened Species. Version 2022-2.
- 957 78. IUCN (International Union for Conservation of Nature) (2016). *Leopardus guttulus*. The IUCN Red
958 List of Threatened Species. Version 2022-2.
- 959 79. European Commission (2021). Tropical Moist Forests product - Resources.
- 960 80. Zhao, T., Zhang, X., Gao, Y., Mi, J., Liu, W., Wang, J., Jiang, M., and Liu, L. (2023). Assessing the
961 Accuracy and Consistency of Six Fine-Resolution Global Land Cover Products Using a Novel
962 Stratified Random Sampling Validation Dataset. *Remote Sensing* 15, 2285.

963

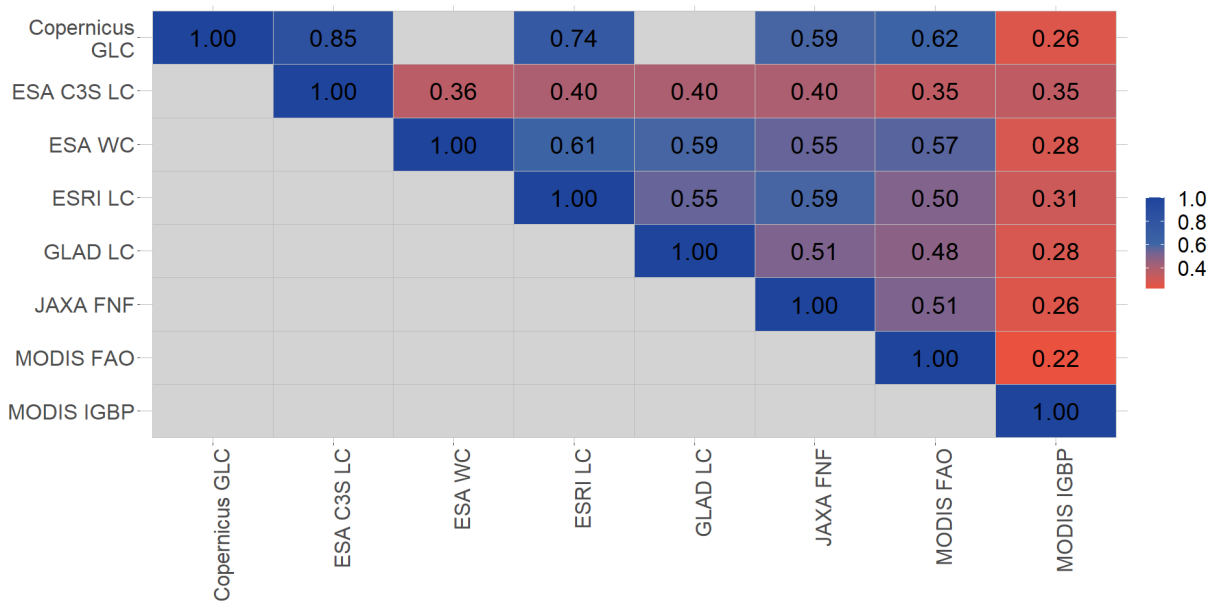
964



966

967

968 **Fig. 1.** (a) Spatial agreement of forest cover classifications between eight land cover datasets.
 969 Spatial agreement is defined as the number of datasets that define a pixel as forest, between 1
 970 and 8. Full agreement between all eight datasets corresponds to a value of eight (dark green), and
 971 no agreement between the datasets corresponds to a value of 1 (dark purple). No color (gray)
 972 indicates that none of the datasets classified the area as forest. All data are from the year 2019
 973 except for ESA-WC and GLAD-LCLUC, which are from 2020. (b) Illustrative case study of a
 974 random area (approximately 16 km²) selected in the country of Colombia showing how the eight
 975 different datasets captured forests and trees differently for the same area. Blue areas are where
 976 the datasets classified land cover as forested.
 977

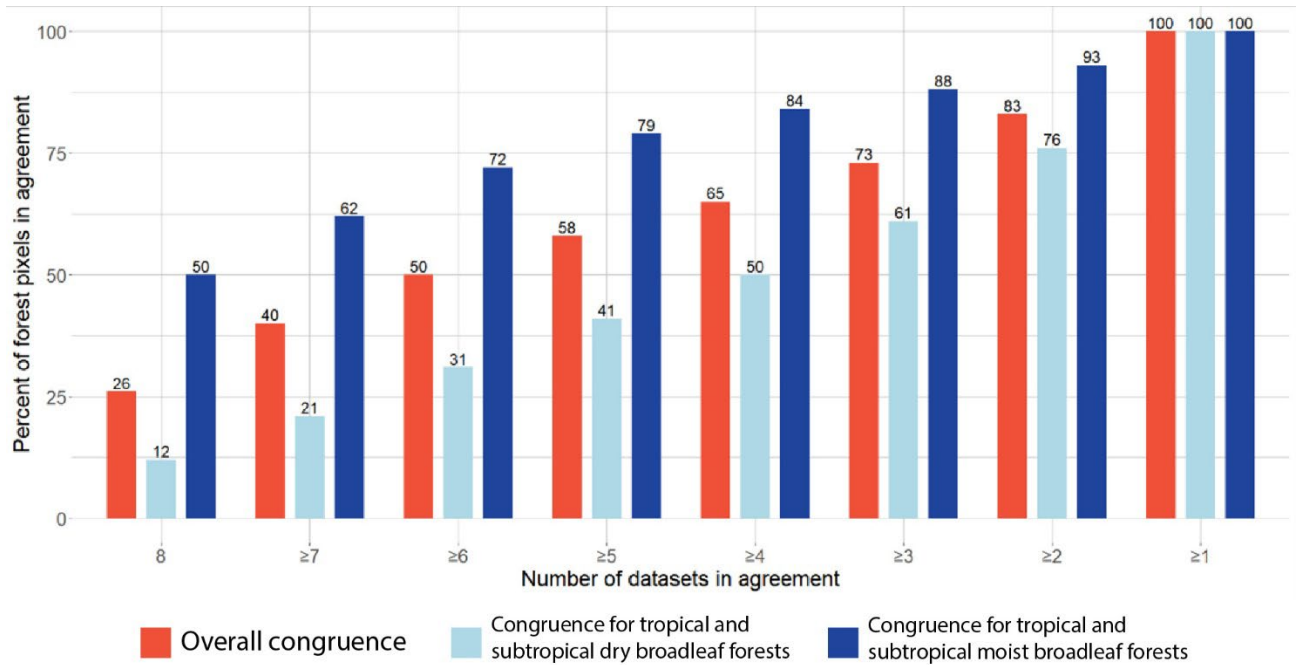


978

979

980 **Fig. 2.** Pairwise agreement between each dataset. CGLC for 2019 is compared to 2019 data for
 981 the other datasets, where available (not available for ESA-WC or GLAD-LCLUC). All other
 982 comparisons are for 2020. Pairwise agreement is defined as the area of intersection where both
 983 datasets agree is forest ($F1 \cap F2$) divided by the total forest area defined by the union of both
 984 datasets ($F1 \cup F2$). Blue indicates high overall spatial agreement between two datasets; red
 985 indicates low overall spatial agreement between two datasets. Pairwise agreement using forest
 986 areas for each individual dataset (showing which forest cover datasets relatively over/under-
 987 estimate forest cover compared to each other) is presented in Table S1.

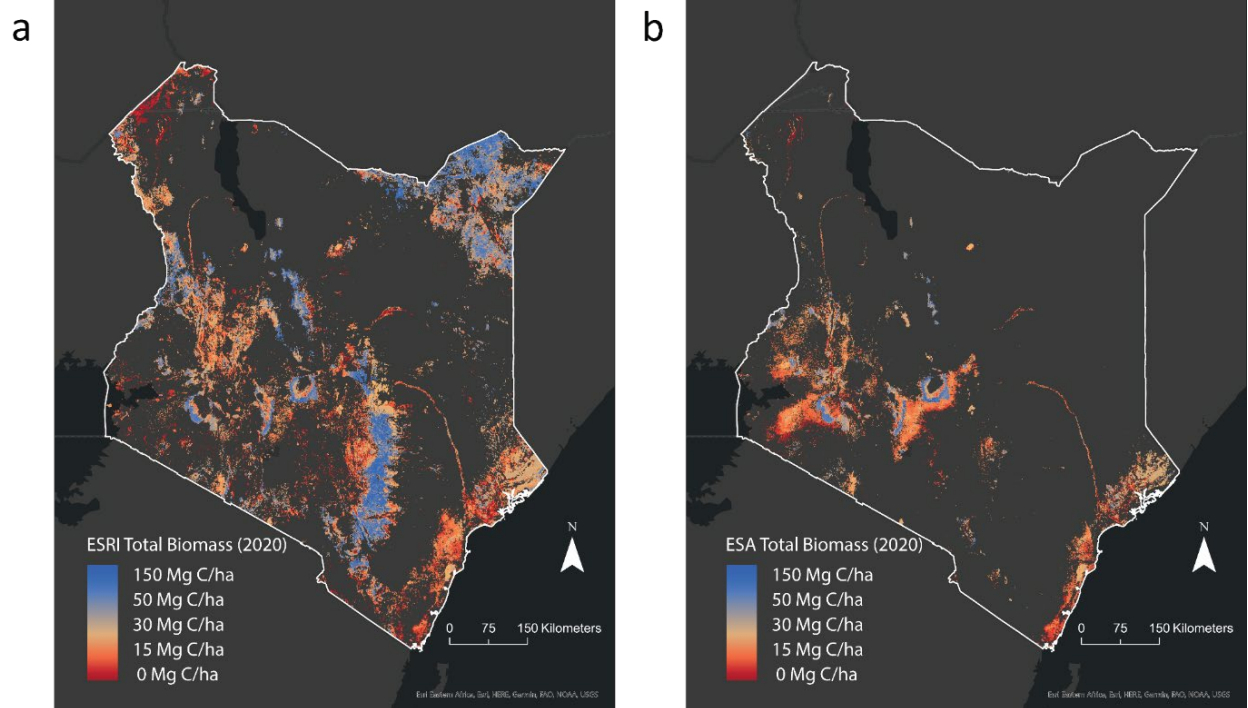
988



989

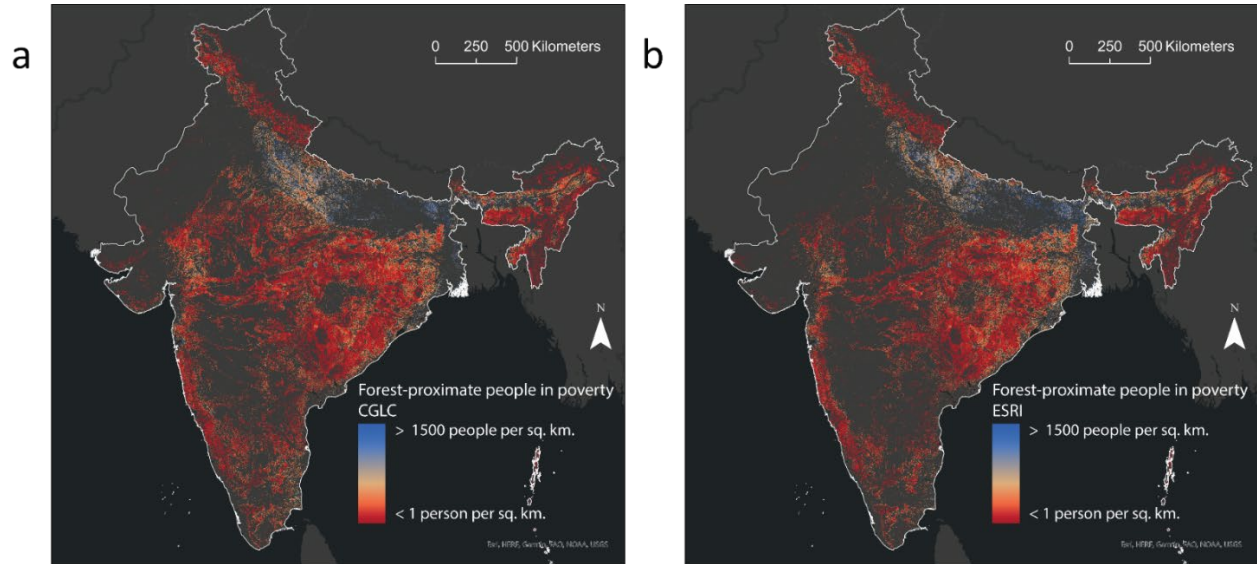
990
991
992
993
994

Fig. 3. Cumulative histogram showing the percent of forest pixels in agreement between the eight datasets globally (leftmost bars, in red) and for two forest biomes, tropical and subtropical dry broadleaf forests (center bars, in light blue), and tropical and subtropical moist broadleaf forests (rightmost bars, in dark blue).



995
 996
 997
 998
 999
 1000
 1001
 1002
 1003
 1004
 1005
 1006
 1007

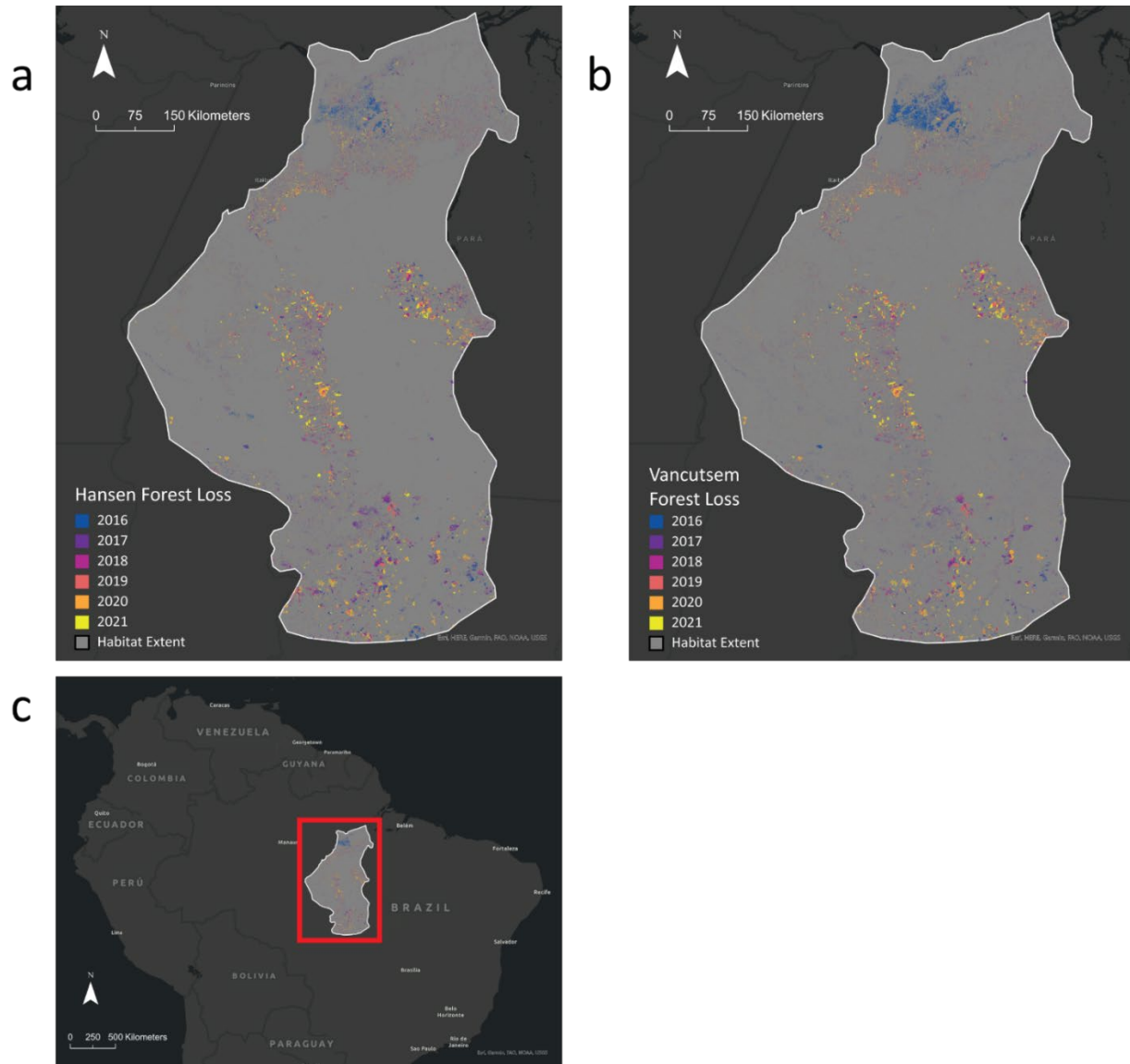
Fig. 4. Estimates of the amount and distribution of forest above- and below-ground carbon biomass in Kenya using two 2020 land/forest cover datasets, (a) ESRI Land Cover, where 26% of total national biomass is located in areas classified as forest; and (b) ESA WorldCover, where 6% of total national biomass is located in areas classified as forest. Total biomass carbon estimates were generated from the Spawn *et al.*³⁵ dataset for the year 2010 and held constant (see Fig. S4 for above-ground and below-ground layers and Fig. S5 for results for all eight GFDs). These maps include the disputed Ilemi Triangle, using the administrative boundaries defined by WorldPop. Note: Carbon density is based on 2010 forest extent and was not updated for 2020. This analysis is illustrative only and intended to show how different GFDs intersect with a fixed carbon map, not to estimate present-day carbon stocks.



1008

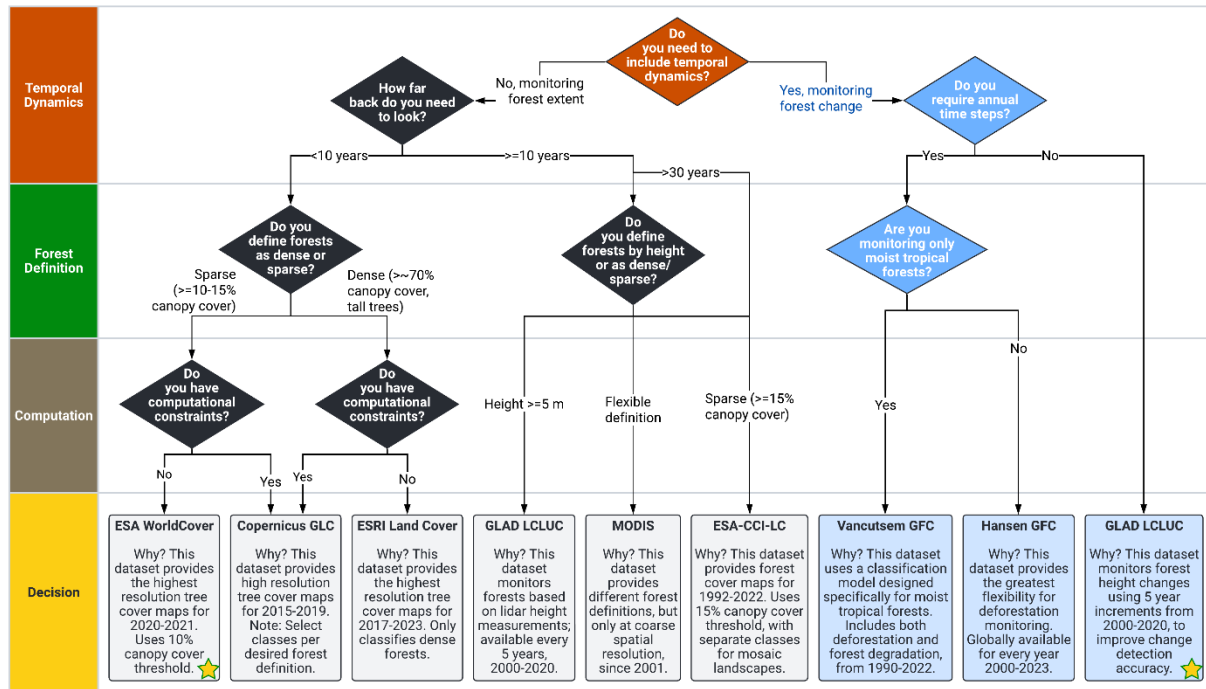
1009
1010
1011
1012
1013
1014
1015
1016
1017

Fig. 5. Estimates of the number of forest-proximate people living in poverty in India in 2016 following the methodology in Newton *et al.*³⁸. We defined forest proximity as people living in or within 1 km of forests, and we defined poverty using the gridded Relative Wealth Index (RWI) published by Chi *et al.*⁷⁴. People living in poverty and in proximity of forests are shown using two different forest cover datasets: (a) Copernicus Global Land Cover (left) and (b) ESA-C3S Land Cover (right). We used country boundaries using the administrative boundaries defined by WorldPop; however, there are several disputed boundaries of India, including the Kashmir region (Aksai Chin and Demchok) as well as Arunachal Pradesh.



1018

1019 **Fig. 6.** Forest cover loss by year between 2016-2021 for (a) Hansen-GFC and (b) Vancutsem-
 1020 TMFCC for the white-cheeked spider monkey's (*Ateles marginatus*) species range. Panel (c)
 1021 shows the region where the white-cheeked spider monkey habitat is located. The Vancutsem-
 1022 TMFCC map includes both forest loss and forest degradation. The map for Vancutsem-TMFCC
 1023 loss data (excluding degraded forest areas) is provided in the supplemental information (Fig. S8).
 1024 Forest gain is not shown in these maps since the Hansen-GFC dataset did not provide annual
 1025 forest gain data.
 1026



★ Recommended as best available, if it meets user's end needs, including regional accuracy.

Note: Users may need to pre-process datasets to remove tree cover that does not meet forest definition (e.g., using a minimum forest area).

1027

1028 **Fig. 7.** Decision tree to help guide dataset selection for different applications. Decision tree branches
 1029 include (1) temporal dynamics: whether the user aims to monitor forest cover or forest cover change; (2)
 1030 forest definition: whether the user defines forests by height, dense canopy cover, or sparse canopy cover,
 1031 or (for forest cover change) whether the user is only monitoring moist tropical forests; and (3)
 1032 computational constraints: whether the user has the computational capacity to run their analysis with very
 1033 high resolution data. The stars indicate the datasets recommended as best available by the authors based
 1034 on our review, if they meet the user's needs. We note that this decision tree does not account for regional
 1035 differences in classification accuracy, which are influenced by factors such as training data, modeling
 1036 approach, and algorithm performance, and varies by world region. Where possible, users should consult
 1037 independent validation studies (e.g.,^{24,28,43,57,80}) to assess which dataset is most appropriate for their
 1038 specific application.